ELSEVIER

Atmospheric Research 37 (1995) 175–209

ATMOSPHERIC RESEARCH

Long-term changes of the diurnal temperature cycle: implications about mechanisms of global climate change

J. Hansen *, M. Sato, R. Ruedy

NASA Goddard Institute for Space Studies, 2880 Broadway, New York, NY 10025 USA

Accepted 17 November 1994

Abstract

We use a global climate model to investigate the impact of a wide range of radiative forcing and feedback mechanisms on the diurnal cycle of surface air temperature. This allows us not only to rule out many potential explanations for observed diurnal changes, but to infer fundamental information concerning the nature and location of the principal global climate forcings of this century. We conclude that the observed changes of the diurnal cycle result neither from natural climate variability nor a globally-distributed forcing, but rather they require the combination of a (negative) radiative forcing located primarily over continental regions together with the known globally-distributed forcing due to anthropogenic greenhouse gases. Tropospheric aerosols can account for part of the continentally-located forcing, but alone they do not damp the diurnal cycle as observed. Only an increase of continental cloud cover, possibly a consequence of anthropogenic aerosols, can damp the diurnal cycle by an amount comparable to observations. A corollary of these results is quantitative confirmation of the widely held suspicion that anthropogenic greenhouse gas warming has been substantially counterbalanced by a forced cooling. Under the assumption that the cloud change is sulfate driven, a further implication is that the net rate of global warming is likely to increase substantially in coming years. We note that, on the long run, the daily maximum temperature will increase by an amount not much less than the increase of the mean temperature.

1. Introduction

Global surface air temperature increased about 0.5°C, or 1°F, in the past century (Hansen and Lebedeff, 1987; IPCC, 1990, 1992; Jones et al., 1991). This observed global warming provides circumstantial evidence in favor of the contention that the greenhouse effect of

* Corresponding author.

SSDI 0169-8095(94)00077-8

anthropogenic trace gases is the dominant global climate forcing mechanism on that time scale. However, the observed global temperature change of that period permits a broad range of interpretations, in part because of the uncertain contribution of unforced climate change, but especially because of the absence of measurements of many potentially significant global climate forcings (Hansen et al., 1993a, b).

One approach toward analysis of the cause of climate change, with potential value even in the absence of measurements of some key climate forcings, is to search for a "fingerprint" of the forcings in the spatial and temporal patterns of observed climate change. Fingerprint studies employing the geographical patterns of surface temperature change have been fruitless, as should be expected given the large natural variability of regional climate and the inability of current models to portray realistically many aspects of regional climate change including changes related to variability of ocean circulation. The fingerprint approach also is limited by the fact that climate models predict rather similar latitudinal and seasonal responses to different forcings, e.g., to increased solar irradiance and increased homogeneously mixed greenhouse gases (Manabe and Wetherald, 1975; Wetherald and Manabe, 1975; Hansen et al., 1984).

Perhaps the most useful fingerprint has been the observation (Angell, 1986, 1991; Oort, 1993; Oort and Liu, 1993) that warming of the past several decades extends upward only to about 12 km altitude, rather than the approximate 16 km altitude expected for climate forcing by only homogeneously mixed greenhouse gases. The lower altitude for the switchover from warming to cooling has been shown to be an expected consequence of ozone depletion in the lower stratosphere (Hansen et al., 1993a). However, the effect of this inferred ozone climate forcing on surface air temperature cannot presently be quantified accurately because of the absence of adequate measurements of the change of the ozone vertical profile (Lacis et al., 1990; Hansen et al., 1993b).

In this paper we study the implications of a different fingerprint in observed climate change, the change of the diurnal cycle of surface air temperature. Karl et al. (1993) examined the change of amplitude of diurnal surface air temperature variations over a large portion (about 37%) of the Earth's land area for 1951–1990, a period encompassing more than half of the global warming of the past century. They found that the amplitude of the diurnal cycle decreased by about 0.5°C, about the same as the mean warming of these same regions for the 1951–1990 period. Changes of the diurnal cycle having the sign and approximate magnitude of the observations were found incidentally in global climate model simulations, using climate forcings based on independent evidence, by Hansen et al. (1993a), but they did not investigate systematically the dependence of the diurnal cycle on individual climate forcings.

Here we examine how the diurnal cycle of surface air temperature is altered by a wide range of different climate forcings, concluding that the observed diurnal changes provide a remarkably strong constraint on the nature of the climate forcings. Specifically, we show that none of the known globally-distributed climate forcings, such as changes of greenhouse gases, stratospheric aerosols, or solar irradiance, can account for the observed diurnal changes. Similarly, global radiative feedbacks, such as a change of clouds and water vapor due to an increasing greenhouse effect, do not produce the observed diurnal changes. Only a forcing concentrated more in the continental regions, such as anthropogenic tropospheric aerosols and aerosol-forced cloud changes, yields a change of the diurnal temperature

amplitude comparable to that observed, and then only in combination with a larger global warming mechanism. Aerosols alone cannot account for the observed damping of the diurnal cycle. Thus the results confirm the existence of a significant cloud radiative forcing, with the simplest interpretation having a net aerosol plus cloud forcing about half as large as the anthropogenic greenhouse gas climate forcing.

2. Observations

We base our present analysis on the observations reported by Karl et al. (1993), supplemented by data of Salinger (1995) for a large region in the Southwest Pacific. The areas represented by the Karl et al. data cover about 50% of Northern Hemisphere land and 10% of Southern Hemisphere land, corresponding to about 37% of global land. Specifically Karl et al. examine the monthly mean maximum and minimum temperatures for these regions for the period 1951–1990. They find that the average minimum temperature increased 0.84°C while the average maximum temperature increased only 0.28°C.

In principle, several parameters could be required to define the diurnal cycle of temperature (Fig. 1). The diurnal cycle can be examined in detail in a global climate model, but available observations are often restricted to maximum and minimum temperatures. The diagnostics of our present climate simulations include the maximum, the minimum, and the true diurnal mean temperature. We find, as shown below, that the difference between the change of (maximum + minimum)/2 and the change of the true mean is generally very small, and thus it is sufficient to deal with two parameters. The mean temperature has been used widely as a climate diagnostic for many years. Thus for the purpose of climate analyses it is most appropriate to choose, as the two parameters, the mean temperature and the amplitude of the diurnal cycle.

Our notation is as follows. T_s is the mean surface air temperature over the diurnal cycle, i.e.,

$$T_s\ (°C) = \text{true diurnal mean.} \tag{1}$$

The (full) amplitude, or range, of the diurnal temperature variation is

$$\text{Amp}\ (°C) = \text{Max} - \text{Min}. \tag{2}$$

The asymmetry of the diurnal cycle is

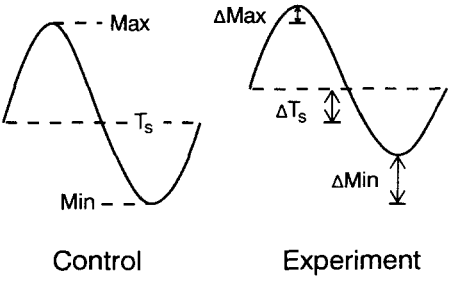

Fig. 1. Schematic indication of parameters used to define the diurnal cycle of surface air temperature.

$$\text{Asym } (°C) = (\text{Max} + \text{Min})/2 - T_s. \quad (3)$$

The Karl et al. (1993) data correspond to a change of mean temperature $\Delta T_s = 0.56°C$ and a diurnal amplitude change $\Delta\text{Amp} = -0.56°C$. Urban effects probably contribute to both the mean warming and the decreased diurnal amplitude, but Karl et al. present evidence, from rural stations, that the urban effects are relatively small. Thus we assume that the mean warming of the nonurban surface air over land is about $0.5°C \pm 0.1°C$ and that the change of amplitude is about $-0.5°C \pm 0.1°C$. The exact values do not affect our conclusions, but in view of the implications inferred from the change of diurnal cycle, it is important to improve knowledge of diurnal change as much as possible. It would be particularly useful to have data on diurnal changes for the land areas not represented in the observations used by Karl et al. (1993). As illustrated by their Fig. 2, and discussed below, the areas with available data are biased toward Northern Hemisphere middle latitudes.

3. Model

Most of our calculations here are carried out with a sector version (120 degrees of longitude) of the GISS climate model II. A sector model, as first employed by Manabe (1969), has a computational efficiency which allows us to explore the effect of many radiative forcings and feedbacks on the diurnal cycle. However, we first show here the geographical and seasonal variation of the amplitude of the diurnal cycle simulated by the full model II, because only that can be compared in detail with observations and because the diurnal cycle was not included in our published model documentation (Hansen et al., 1983).

The amplitude of the diurnal cycle in model II and observations is shown in Fig. 2 for January and July. Differences between the model and observations are apparent, especially a tendency for the diurnal amplitude to be too large in the summer. However, the model does give about the observed magnitude of the diurnal cycle amplitude, including seasonal and latitudinal variations. Thus we anticipate that changes to the diurnal cycle calculated to result from specified changes in radiative forcings, which are represented in model II with some precision (Hansen et al., 1983), should be reasonably realistic, especially when averaged over large areas.

The geography of the sector ("Wonderland") version of model II is chosen such that the amount of land as a function of latitude is the same as on Earth (Fig. 3). The land masses have fictitious names to help keep emphasis on the purposes for which the model is intended, that is, analysis of climate mechanisms, rather than on climate impacts in specific real world regions, which are often subject to overinterpretation. This is particularly relevant to analysis of the diurnal cycle, which is influenced by many unpredictable local and regional climatic factors, but nevertheless carries substantial information in its large scale changes.

The zonal mean climate of the Wonderland model is very similar to that of the full model II. We illustrate here only the zonal mean temperature, zonal wind and mass stream function (Fig. 4). The resolution used for the Wonderland model is $7.86 \times 10°$ (Fig. 3) with nine layers in the atmosphere, as in the documented version of model II (Hansen et al., 1983). The winter low level temperature inversion at high latitudes is too weak in the Wonderland

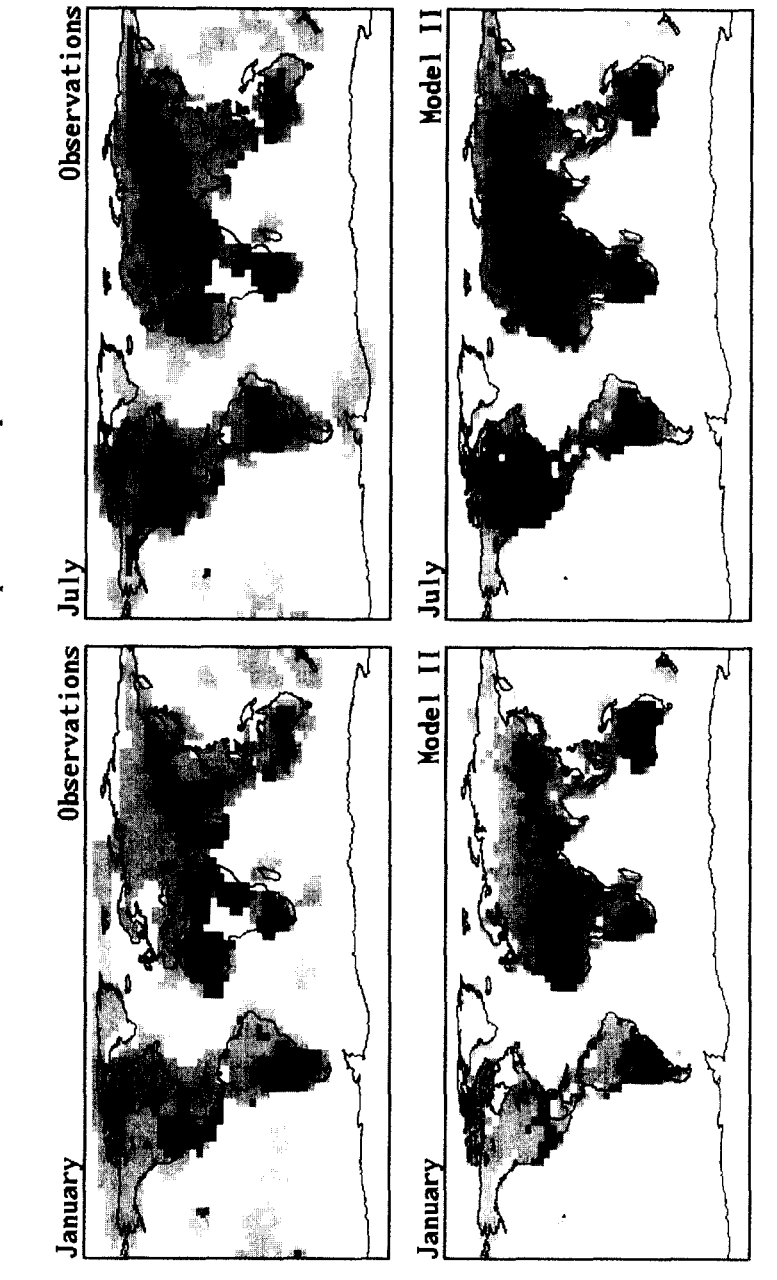

Fig. 2 Amplitude of diurnal cycle of surface air temperature in observations for January and July reported by May et al. (1992) and as simulated by GISS model II.

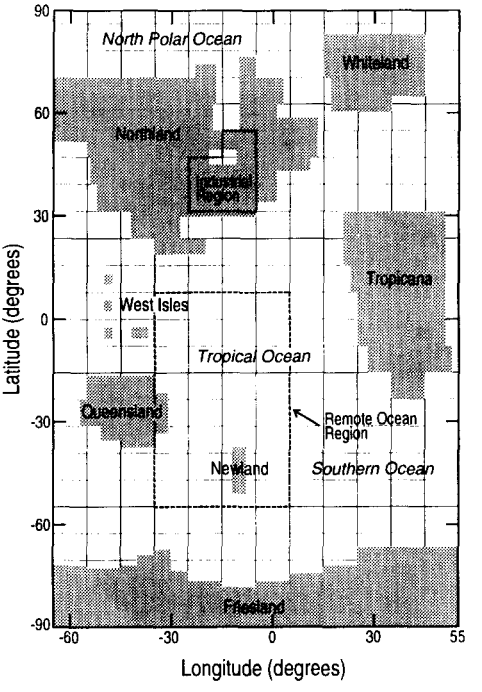

Fig. 3. Geography of Wonderland. The GCM computational grid is indicated.

model and the summer high latitude stratosphere is too cold, the latter problem shared with many other models. The meridional circulation, in both the Hadley and Ferrel cells, is weaker than observed, but similar to model II. A more comprehensive documentation of the Wonderland model is in preparation (Hansen et al., 1995a).

In addition to the above standard version of the Wonderland model, we have used other versions of the model in which specific feedback processes are prohibited from operating, for example, either the clouds or the sea ice being held fixed. The purpose of these alternate versions is to allow us to study the role of each feedback process in affecting climate sensitivity, as well as to provide information on how atmospheric and surface processes affect the diurnal cycle of surface air temperature.

All these versions of the model have an ocean mixed layer of seasonally varying depth with specified horizontal heat transports (Hansen et al., 1993a, 1995a). As in the model described by Hansen et al. (1984), the ocean heat transports are obtained as the implicit ocean transports in the first control run of the model, which has specified seasonally varying sea surface temperatures.

Because we find that cloud changes must be a key factor causing observed changes of the diurnal cycle of surface air temperature, let us clarify how clouds are calculated or specified in the Wonderland model. Calculated clouds have the same properties as in model II (Hansen et al., 1983), with the optical thickness fixed as a function of model layer and clouds prohibited from occurring in the top two layers of the model (above 150 mb). "Fixed clouds" were obtained by saving the computed clouds at every time step, gridbox and

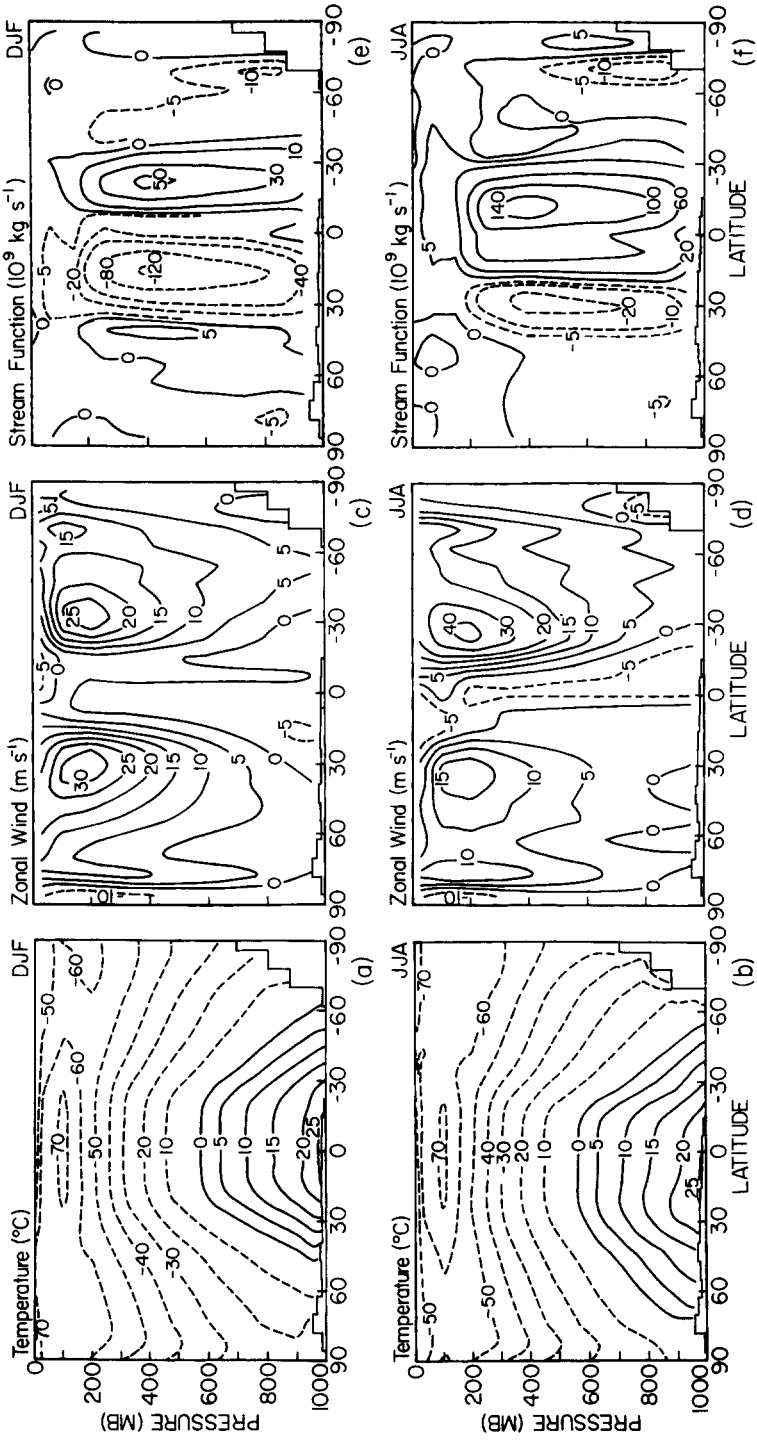

Fig. 4. Zonal mean temperature (a, b), zonal wind (c, d) and mass stream function (e, f) in the Wonderland model control run (years 51–100). The upper figures are for Dec–Jan–Feb and the lower for Jun–Jul–Aug. Compare to observations and model II results in figs. 20, 29 and 31 of Hansen et al. (1983).

atmospheric level in one year of the model control run with computed clouds. Thus in the experiments with fixed clouds, the clouds vary spatially, diurnally and seasonally, but they are the same every year and they are the same in the relevant control run as in the experiment runs. Although clouds are not allowed to change as a climate feedback mechanism in the model with fixed clouds, in some experiments we insert specified cloud changes at particular levels or geographic locations in order to determine their influence on the diurnal cycle. This approach for analyzing the relation between clouds and the diurnal cycle is dictated by the large uncertainty in the nature of anthropogenically forced cloud changes as well as by our inability as yet to model clouds reliably as a climate feedback mechanism.

4. Control runs

The global mean temperature in 200 year periods of four control runs is shown in Fig. 5. Variability of temperature is largest when all feedbacks are allowed to operate, as expected since in the model both sea ice and clouds are positive feedbacks (Hansen et al., 1984).

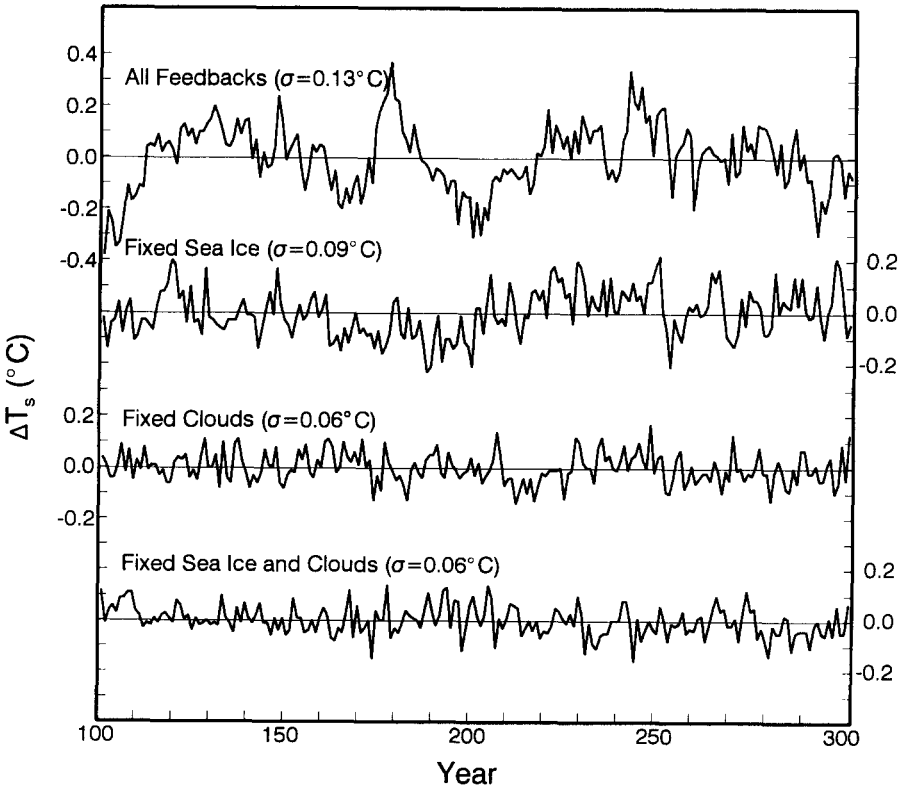

Fig. 5. Annual-mean global-mean surface air temperature in four control runs of the Wonderland model. Each of the runs had a 100 year spin-up, and the temperature illustrated is the deviation from the 101–300 year mean. σ is the standard deviation about this 200 year mean. The run with all feedbacks included was run an additional 600 years (Fig. 8); the standard deviation for the full 800 years is also $\sigma = 0.13$°C.

The standard deviation of annual-mean global-mean surface air temperature is 0.13°C in the case with all feedbacks, 0.09°C with fixed sea ice, 0.060°C with fixed clouds, and 0.058°C with fixed sea ice and clouds.

Analysis of surface air temperature variability in the standard version (all feedbacks included) of the Wonderland model (Miller and DelGenio, 1994) has shown that part of the variability is associated with a positive interaction between low latitude sea surface temperature fluctuations and cloud cover, which is at least partly an unrealistic aspect of the cloud parameterization in model II. Additional variability is associated with a positive interaction between sea ice fluctuations and local cloud cover. These positive interactions, or feedbacks, among the global climate feedbacks are manifested in the standard deviations given above for the four control runs in Fig. 5. Because of uncertainty about the realism of modeled cloud feedbacks, our analyses of the diurnal cycle use both fixed cloud and calculated cloud models.

The simulated amplitude of the diurnal cycle of surface air temperature, Amp, is shown in Fig. 6 for two control runs of the Wonderland model. Amp depends relatively little on whether the radiative feedbacks, including water vapor change (not illustrated), are allowed to operate or not allowed to operate.

Kukla and Karl (1993) ask whether the observed near-global decrease of Amp by about 0.5°C could be a result of natural climate variability. Certainly large changes of ΔAmp can occur with regional climate change, as a result of changes of such factors as soil moisture, evaporation, snow cover and cloud cover. We have looked at the unforced variability of Amp in the global climate models in several ways. First, because one might expect large global changes of Amp to occur in conjunction with extreme global temperatures, we compared Amp in cool and warm decades of the control run with all feedbacks allowed to operate. Fig. 7 shows the change of the diurnal amplitude from cool to warm periods, for which the corresponding global mean surface air temperature changes were about 0.3°C. Substantial changes of the diurnal amplitude, a large fraction of a degree, occur in any given region. Some of the diurnal changes over land are associated with long-term fluctuations of soil moisture, while the largest diurnal changes over ocean are in association with fluctuations of sea ice cover. Thus it is clear that considerable interannual and long-term changes of the amplitude of the diurnal cycle can occur regionally without any climate forcing. However, the changes of Amp averaged over all land were found to be only -0.09 and -0.08°C for the intervals illustrated in Fig. 7.

Fig. 8 shows the interannual and decadal changes of Amp over land and global T_s for 800 years of the control run with all feedbacks allowed to operate. There is some (negative) correlation of Amp over land with global T_s, as expected, since the amount of water vapor over land tends to increase with higher global temperature. Other mechanisms can be examined via Fig. 9 which shows changes of several quantities between two decades having a large difference of Amp averaged over global land. The largest regional variations of Amp are associated with changes of soil moisture, evaporation and cloud cover. However, the largest change of Amp between any two decades, averaged over global land, is only about 0.2°C, and the trend over any 40 year period is considerably less.

We conclude that observed changes of Amp over land by 0.5°C cannot be a result of unforced variability unless there are mechanisms of variability several times larger than those in our model, which seems to us to be unlikely. In particular, we note that potential

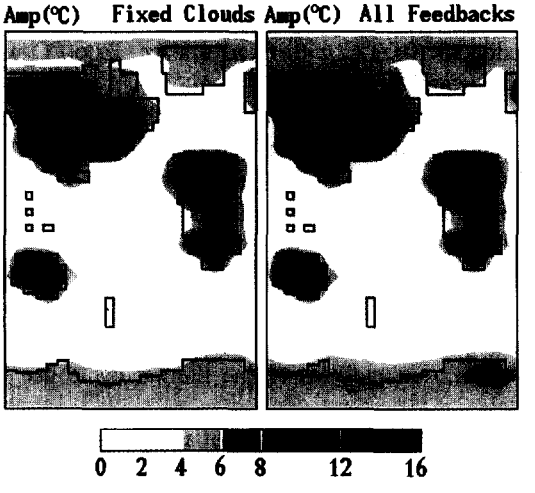
Amp(°C) Fixed Clouds
Amp(°C) All Feedbacks
0 2 4 6 8 12 16

Fig. 6

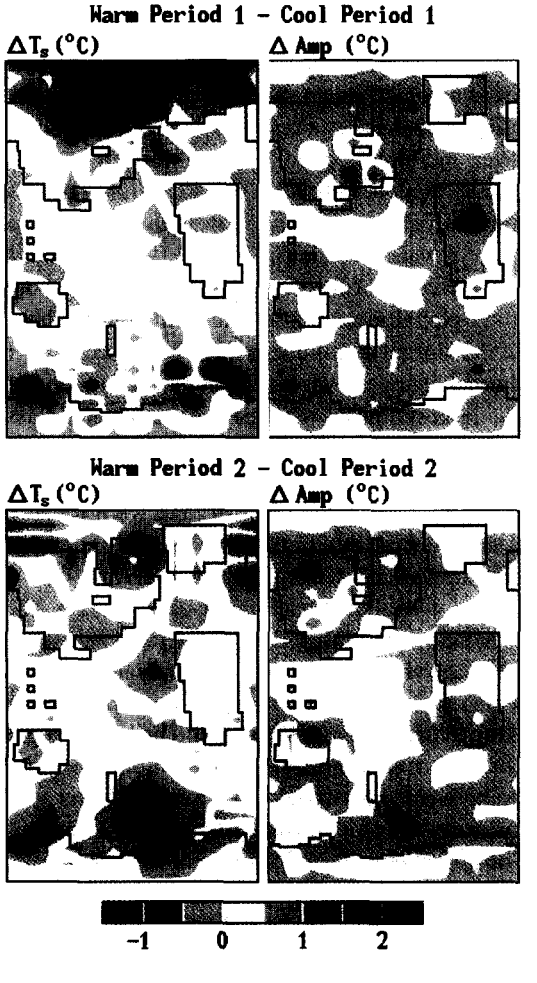
Warm Period 1 - Cool Period 1
ΔTs (°C)
Δ Amp (°C)
Warm Period 2 - Cool Period 2
ΔTs (°C)
Δ Amp (°C)
-1 0 1 2

Fig. 7

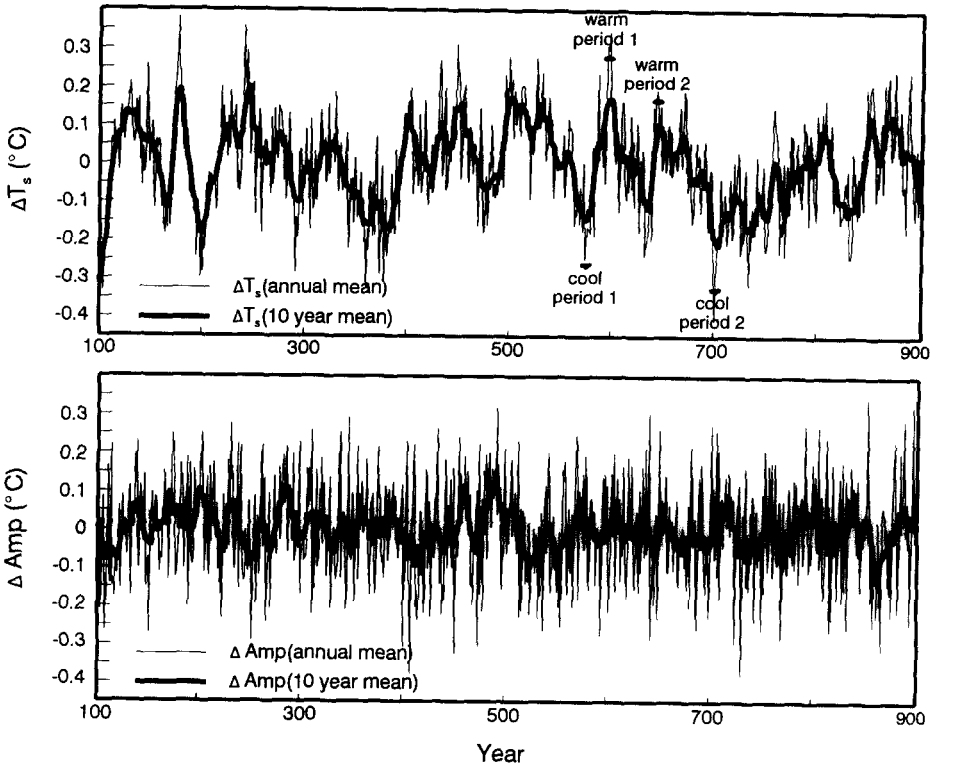

Fig. 8. Annual and 10-year running mean changes of Amp over land for the control run of the Wonderland model with all feedbacks allowed to operate. The change of global mean temperature is shown for comparison.

changes of ocean circulation, excluded in our current model, would alter the diurnal cycle through the same atmospheric and surface mechanisms as in the present model; thus, although ocean circulation changes could alter geographical patterns of Amp, we would not expect them to cause large changes of the global mean value.

The conclusion that the observed global trend of Amp cannot be explained by unforced variability does not imply that such fluctuations of Amp are negligible. The above results show significant decadal fluctuations, even on the global scale. Unforced variability is sufficient to account for large regional differences in decadal trends, and it must contribute to observed regional differences from the mean Karl et al. (1993) trend of Amp. Regional anomalies, such as the increasing values of Amp reported for India by Kumar et al. (1994), may be related to regional climate fluctuations.

Fig. 6. Annual mean amplitude of the diurnal cycle of surface air temperature in two control runs of the Wonderland model.

Fig. 7. Change of T_s and Amp between cool and warm periods in the control run with all feedbacks operating (see Fig. 8). The maps show the differences: warm period 1 minus cool period 1, and warm period 2 minus cool period 2.

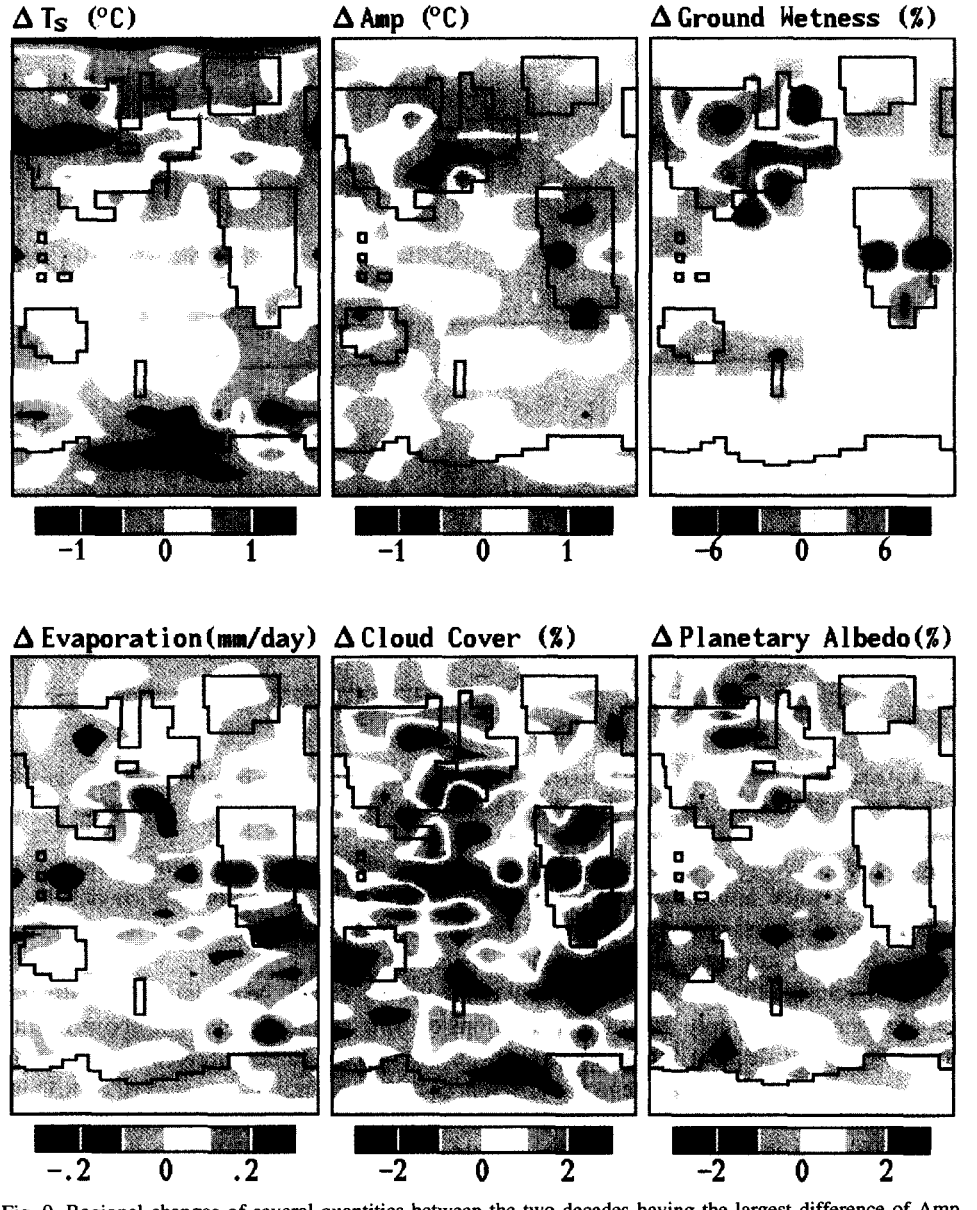

Fig. 9. Regional changes of several quantities between the two decades having the largest difference of Amp averaged over land in the Wonderland control run in which all feedbacks are allowed to operate. The quantities illustrated are surface air temperature, diurnal amplitude of surface air temperature, ground wetness, evaporation, cloud cover and planetary albedo. Changes are for years 521–530 minus years 481–490.

5. $2\times CO_2$ and $\pm 2\%$ S_o experiments

It is instructive to examine first the change of diurnal cycle for the climate forcings used by Manabe and Wetherald in their classical experiments (Manabe and Wetherald, 1975;

Wetherald and Manabe, 1975): a doubling of atmospheric carbon dioxide and a two percent change of solar irradiance. For intercomparison of these and other forcings it is useful to specify the magnitude of all forcings in the same units. For that purpose we choose the instantaneous forcing, defined as the radiative flux change at the 150 mb level, approximately the tropopause, in a one year run of the model with the radiative forcing mechanism inserted but with all global properties including temperature held fixed. Elsewhere (Hansen et al., 1995b) we illustrate quantitatively the merits of alternative measures of climate forcing. The instantaneous flux change at 150 mb is an adequate measure of climate forcing for the purposes of analyzing changes of the diurnal cycle.

Global maps of this climate forcing are shown in Fig. 10a for the $2\times CO_2$ and $+2\%\ S_0$ experiments. The $2\times CO_2$ forcing is much more globally uniform than the $+2\%\ S_0$ forcing, which is more concentrated toward low latitudes. The forcing for $-2\%\ S_0$ is the negative of that for $+2\%\ S_0$.

The equilibrium surface air temperature change is shown in Fig. 11 for all three forcings ($2\times CO_2$, $+2\%\ S_0$ and $-2\%\ S_0$) for two versions of the model (fixed clouds and the

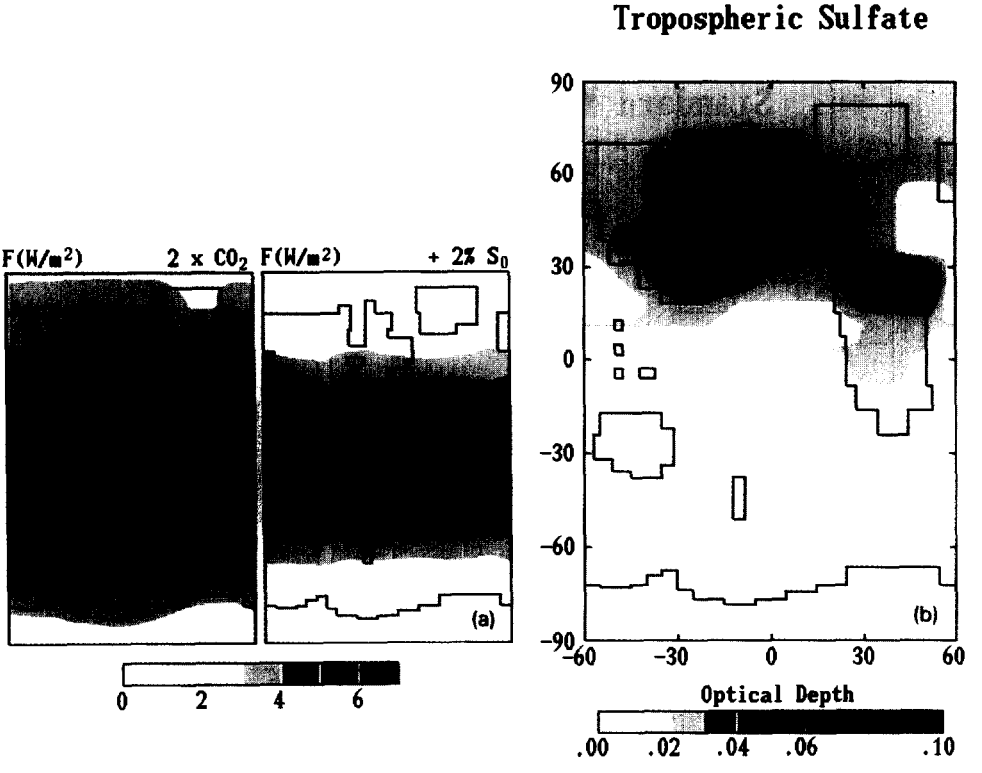

Fig. 10. (a) Climate forcing for $2\times CO_2$ and $+2\%\ S_0$ experiments, defined as the instantaneous radiative flux change at the 150 mb level. This is the flux change obtained in a one year run of the model with the forcing inserted but all climate parameters including temperature held fixed. (b) Geographical distribution of aerosol optical depths in the Wonderland model for the fourth case of Fig. 18. This is the same distribution used by Hansen et al. (1993a), based on the anthropogenic sulfate global and zonal amounts of Charlson et al. (1991), using an analogous spatial dispersion over land at the same latitudes of Wonderland.

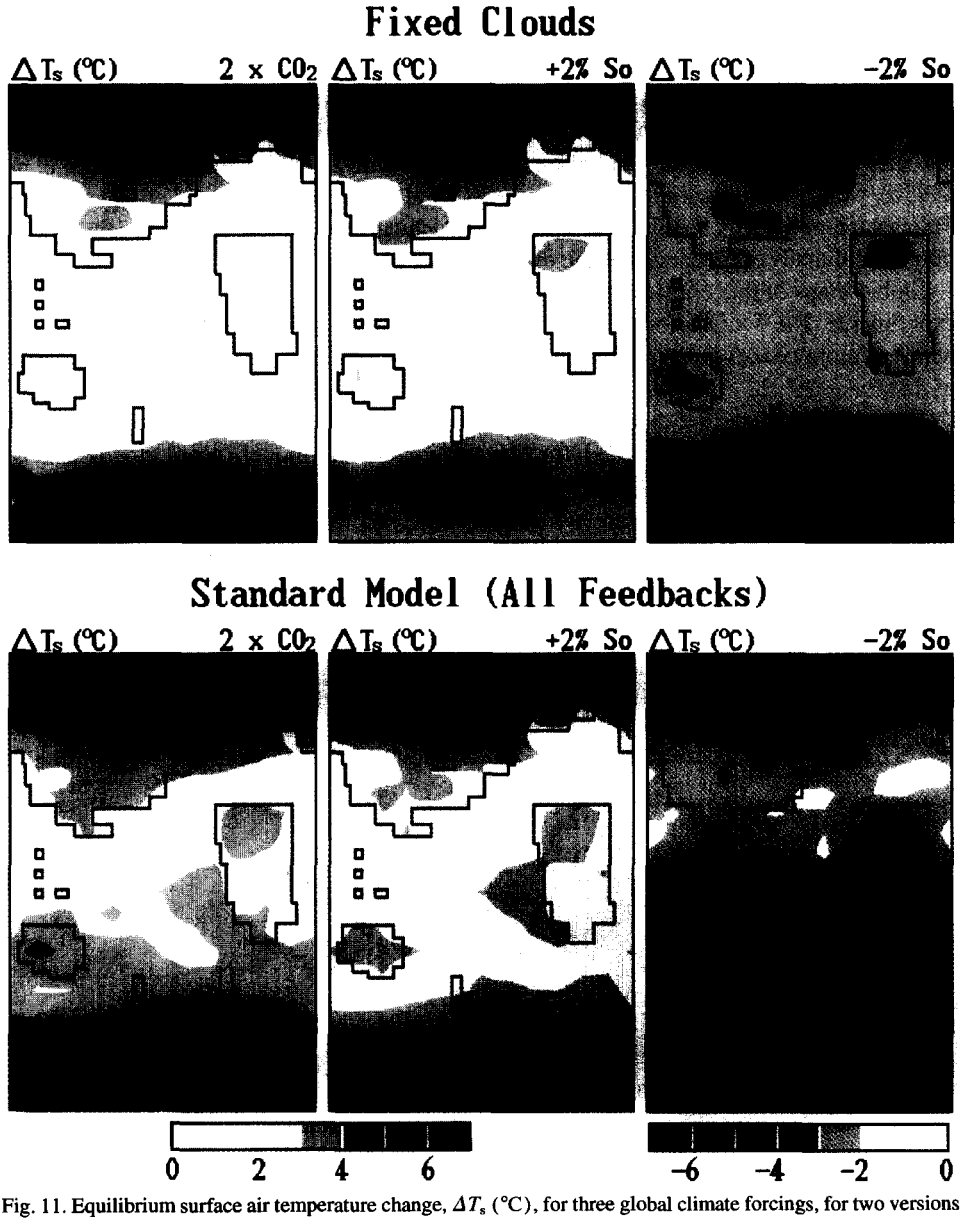

Fig. 11. Equilibrium surface air temperature change, ΔT_s (°C), for three global climate forcings, for two versions of the Wonderland model.

standard version of the model with all feedbacks operating). The experiments were run 130 years, with the equilibrium response defined as the mean for years 71–130. Additional feedbacks, other than clouds, and their interactions are examined by Hansen et al. (1995b). We note here only that there is a reinforcing interaction between the sea ice and cloud feedbacks, which increases toward colder climates as greater regions of sea ice come into

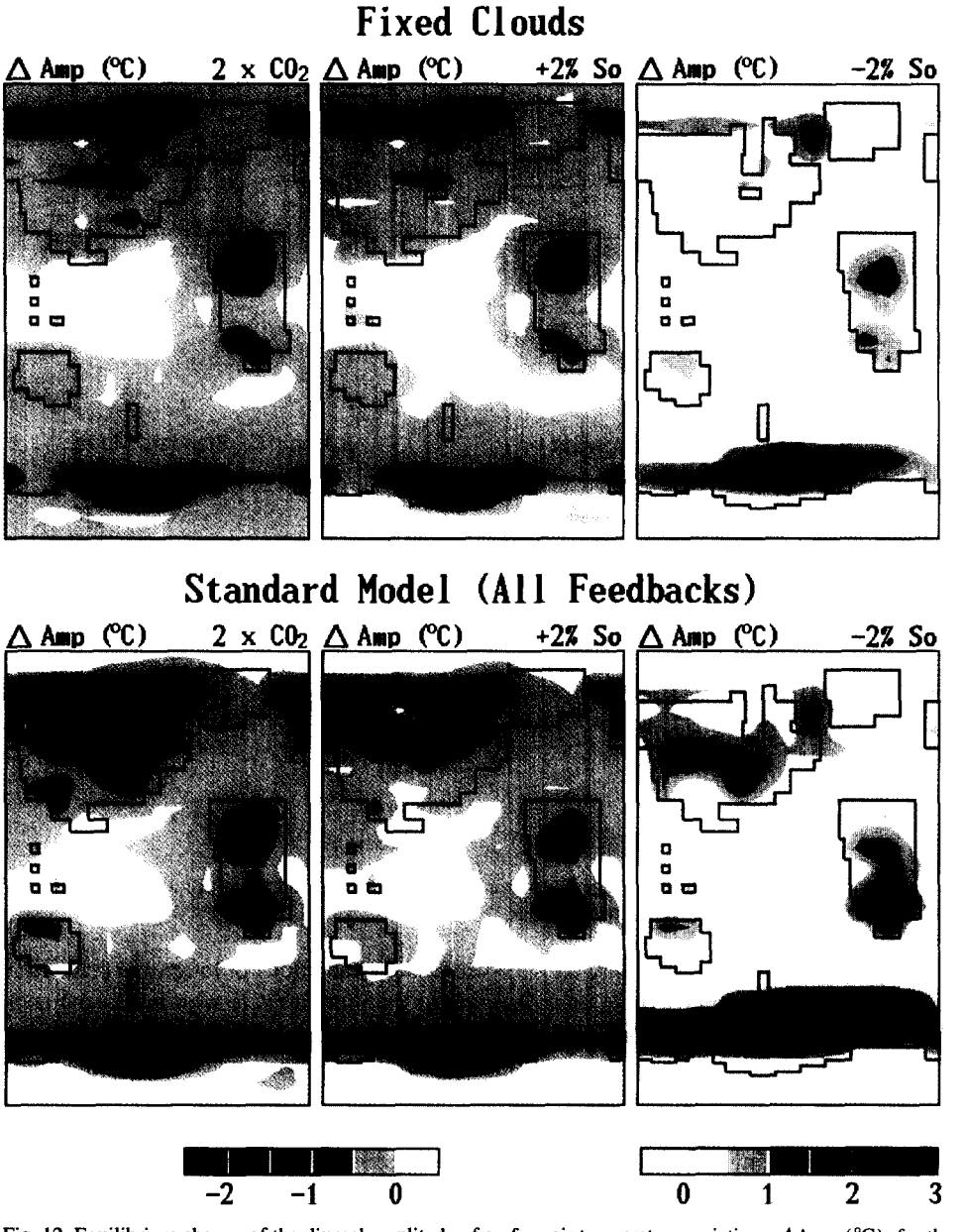

Fig. 12. Equilibrium change of the diurnal amplitude of surface air temperature variations, ΔAmp (°C), for the same three climate forcings and two versions of the Wonderland model as in Fig. 11.

play, as is most evident in the Southern Hemisphere in the -2% S_0 experiment. We do not know whether this interaction is realistic, but it does not significantly affect our conclusions in this paper, which are based on observed changes of the diurnal cycle over land.

The change of the amplitude of the diurnal cycle for these same six experiments is shown in Fig. 12. Solar irradiance change is an example of a forcing which does not itself alter the

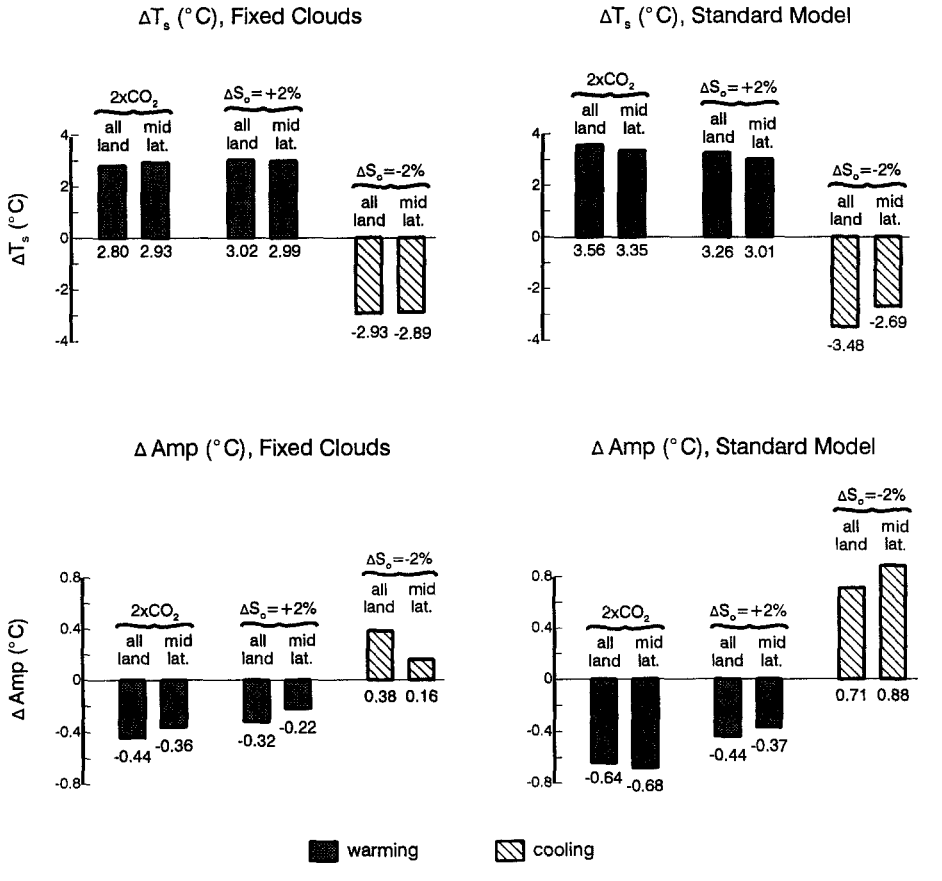

Fig. 13. Equilibrium response of surface air temperature parameters T_s (°C) and Amp (°C) in two versions of the Wonderland model for three global climate forcings.

opacity of the atmosphere in either the shortwave (solar radiation) or longwave (terrestrial radiation) spectral region. The global damping of the diurnal cycle with increasing solar irradiance is primarily a result of increasing atmospheric water vapor, which reduces nighttime cooling. The damping is larger over land than over open ocean. The largest damping occurs where sea ice cover decreases. Doubled carbon dioxide increases the damping of the diurnal cycle compared to increased solar irradiance, because carbon dioxide itself increases the atmospheric longwave opacity, but the carbon dioxide impact is much less than that of water vapor.

Fig. 13 and the first six lines of Table 1 summarize the changes of T_s and Amp averaged over all land in Wonderland (excluding the ice sheets of Friesland and Whiteland), averaged over all land at latitudes 31–55N (the latitudes where the largest number of real world observations are available), averaged over the Industrial Region of Northland (where, in some experiments, the forcing is more concentrated), and averaged over a remote ocean region at low and southern latitudes (analogous to a region in the real world with observations reported by Salinger, 1995). These regions, identified in Fig. 3, provide some

Table 1

Equilibrium changes of surface air temperature and diurnal cycle parameters in GCM experiments with a variety of globally uniform radiative forcings. All of these experiments have fixed clouds except the three experiments indicated as "all feedbacks." The "land" results refer to the mean for all land in Wonderland excluding the ice-covered continents Whiteland and Friesland. Ozone changes are for addition of 0.1 cm-atm in each layer, but $^{n}\Delta$Amp and $^{n}\Delta$Asym are scaled to represent the changes of Amp and Asym for a doubling of the climatological ozone amount in the indicated layers (0.001, 0.005, 0.013 and 0.034 cm-atm in layers 1, 4, 7 and 10, respectively. τ is optical depth, ϖ is single scattering albedo, and ghg is greenhouse gases

Experiment	F_{inst}	ΔT_s			ΔAmp	$^{n}\Delta$Amp				$^{n}\Delta$Asym
		Global	SH-NH	All land	All land	All land	Mid lat.	Indus. region	Remote ocean	All land
$2\times CO_2$ (fixed clouds)	4.35	2.70	−0.17	2.80	−0.44	−0.08	−0.06	−0.09	−0.02	0.013
+2% S_o (fixed clouds)	4.39	2.88	−0.14	3.02	−0.32	−0.05	−0.04	−0.03	−0.01	0.014
−2% S_o (fixed clouds)	−4.39	−3.05	−0.51	−2.93	0.38	0.06	0.03	0.04	0.01	−0.013
$2\times CO_2$ (all feedbacks)	4.35	3.64	0.39	3.56	−0.64	−0.09	−0.09	−0.12	−0.01	0.014
+2% S_o (all feedbacks)	4.39	3.22	0.27	3.26	−0.44	−0.07	−0.06	−0.06	−0.01	0.015
−2% S_o (all feedbacks)	−4.39	−4.70	−3.41	−3.48	0.71	0.10	0.13	0.17	0.04	−0.015
Ghost (surface)	4.00	2.82	−0.20	3.03	−0.69	−0.11	−0.09	−0.10	—	0.019
Ghost (layer 1)	4.00	2.89	−0.16	2.95	−0.36	−0.06	−0.04	−0.03	—	0.012
Ghost (layer 4)	4.00	2.44	−0.10	2.53	−0.37	−0.07	−0.04	−0.05	—	0.016
Ghost (layer 7)	4.00	2.34	−0.18	2.55	−0.37	−0.07	−0.05	−0.05	—	0.019
Ghost, 8W/m^2 day (layer 1)	4.00	2.84	−0.14	2.91	−0.29	−0.05	−0.03	−0.03	—	0.015
Ghost, 8W/m^2 night (layer 1)	4.00	2.91	−0.19	3.04	−0.43	−0.07	−0.05	−0.04	—	0.009
Ozone (0.1 cm-atm in layer 1)	0.23	0.18	−0.01	0.27	−0.39	−0.00	−0.00	−0.00	—	0.001
Ozone (0.1 cm-atm in layer 4)	2.00	1.24	0.00	1.26	−0.37	−0.02	−0.01	−0.01	—	0.003
Ozone (0.1 cm-atm in layer 7)	4.66	1.83	−0.11	1.99	−0.29	−0.04	−0.03	−0.03	—	0.010
Ozone (0.1 cm-atm in layer 10)	−0.69	−0.16	−0.04	−0.15	−0.02	−0.01	−0.01	−0.01	—	0.007
no trop. aerosols	2.61	1.59	0.13	1.59	0.02	0.01	0.03	0.07	—	0.005
trop. aerosols $\Delta\tau=0.1$, $\varpi=1$	−2.44	−1.55	−0.11	−1.53	0.15	0.05	0.01	0.03	0.01	−0.011
strat. aerosols $\Delta\tau=0.1$, $\varpi=1$	−3.09	−1.76	−0.24	−1.71	0.21	0.06	0.02	0.01	—	−0.018
+5% clouds (layer 1)	−5.60	−3.85	−0.53	−3.63	0.19	0.03	−0.02	−0.03	—	−0.015
+5% clouds (layer 4)	−3.01	−1.65	−0.10	−1.61	0.03	0.01	−0.03	−0.04	−0.01	−0.013
+5% clouds (layer 6)	0.76	0.49	0.06	0.47	−0.10	−0.10	−0.06	−0.01	−0.04	0.016
+5% clouds (layer 7)	1.25	0.71	−0.03	0.75	−0.12	−0.08	−0.03	−0.01	−0.02	0.014
Greenhouse gases only	2.38	1.58	−0.01	1.61	−0.27	−0.08	−0.07	−0.07	−0.02	0.013
ghg + sulfate ($\Delta\tau=0.057$, $\varpi=1$)	0.99	0.65	0.05	0.67	−0.15	−0.11	−0.08	−0.07	−0.05	0.015
ghg + low clouds (Δgcc = 1.2%)	1.00	0.67	0.03	0.68	−0.21	−0.15	−0.15	−0.19	−0.02	0.011
ghg + mid clouds (Δgcc = 2.3%)	1.00	0.77	0.06	0.79	−0.26	−0.16	−0.16	−0.21	−0.07	0.013

indication of the spatial inhomogeneity of the response, and are helpful for specific discussions later in the paper.

Several conclusions are suggested by these experiments and supported by experiments for a number of additional radiative forcings as described later in this paper and by Hansen et al. (1995b). Changes of T_s and Amp are reasonably linear as a function of the forcing over a range of forcing ($\pm 2\%$ S_0) which is at least as great as that occurring in the past century. The main nonlinearity occurs in the standard model (all feedbacks allowed) in the region of Southern Hemisphere sea ice, where the sea ice and cloud feedbacks reinforce each other and are more effective for a colder climate with more sea ice. A corollary is that changes in Amp for a given type of forcing are approximately proportional to the calculated equilibrium global temperature change, so we can estimate changes of Amp for smaller forcings by reducing the calculated values in proportion to the global temperature change.

Let us define the normalized changes of the amplitude and asymmetry of the diurnal cycle as the calculated changes reduced to their values for a global warming of 0.5°C, i.e.,

$$^{n}\Delta\mathrm{Amp} = \Delta\mathrm{Amp} \times [0.5/|\Delta T_s|] \tag{4}$$

and

$$^{n}\Delta\mathrm{Asym} = \Delta\mathrm{Asym} \times [0.5/|\Delta T_s|], \tag{5}$$

where ΔT_s is the surface air temperature change averaged over all land excluding the ice sheets of Whiteland and Friesland. As summarized in Table 1, the calculated damping of the diurnal cycle corresponding to a global warming of 0.5°C is only about 0.1°C for either solar irradiance or CO_2 changes, far smaller than the observed ΔAmp of about 0.5°C.

A principal conclusion of these experiments is that the change of atmospheric opacity associated with plausible carbon dioxide and solar irradiance forcings is much too small to decrease the amplitude of the diurnal cycle by 0.5°C. This is consistent with the earlier doubled carbon dioxide experiment of Cao et al. (1992), who obtained an even smaller damping of the diurnal cycle. We show below that this result is general to a much larger group of climate forcings, provided that the forcings are distributed globally, i.e., with the same optical depth over ocean as over land. The calculated damping of the diurnal cycle, less than 0.1°C averaged over all land areas, is primarily a result of the atmospheric water vapor increase associated with a global warming of 0.5°C. The added effect of carbon dioxide opacity itself is small, still leaving the total damping at less than or about 0.1°C. This result does not depend upon whether or not cloud feedbacks are allowed to operate in the model. Of course the result must be qualified by the caveat that the real world may have changing sources of atmospheric opacity other than those included in our model, or those in our model may be unrealistically simulated. But the huge discrepancy with the observed ΔAmp, more than a factor of five, makes model deficiencies an unlikely explanation.

Another conclusion of these simulations and those described below is that changes of Asym, when scaled to their values for global temperature change of 0.5°C or less, are small (Tables 1 and 2). Thus the two parameters T_s and Amp can adequately describe the diurnal temperature change.

6. Other global forcings

We have carried out simulations with the Wonderland model using a large number of additional climate forcings. Fig. 14 and Table 1 summarize the equilibrium change in the

Table 2
Equilibrium changes of surface air temperature and diurnal cycle parameters in GCM experiments with a variety of inhomogeneously distributed radiative forcings. The greenhouse gas changes are globally uniform, while the aerosol and cloud changes are uniform over all land (about 30 percent of global area) and zero over the ocean, except in the final two experiments, in which the geographical distribution of the sulfate and cloud changes follows Fig. 10b. All of these experiments have fixed clouds except the second greenhouse gas plus sulfate experiment, which allowed all model feedbacks to operate. The "land" results refer to the mean for all land in Wonderland excluding the ice–covered continents Whiteland and Friesland

Experiment	F_{inst}	ΔT_s			ΔAmp	$^n\Delta$Amp				$^n\Delta$Asym
		Global	SH-NH	All land	All land	All land	Mid lat.	Indus. region	Remote ocean	All land
sulfate $\Delta\tau=0.33$	−1.84	−1.09	0.52	−1.45	−0.03	−0.01	−0.09	−0.12	0.01	−0.005
+3% clouds (layer 1)	−2.59	−1.51	0.66	−1.90	−0.37	−0.10	−0.18	−0.25	0.02	−0.012
+3% clouds (layer 4)	−1.20	−0.52	0.07	−0.44	−0.35	−0.39	−0.58	−0.83	0.05	−0.005
+3% clouds (layer 7)	0.77	0.48	−0.02	0.51	−0.11	−0.11	−0.09	−0.16	−0.03	0.014
ghg + sulfate ($\Delta\tau=0.25$)	0.99	0.73	0.43	0.51	−0.27	−0.27	−0.33	0.32	−0.06	0.027
ghg + sulfate (all feedbacks)	0.99	1.33	0.88	0.93	−0.40	−0.21	−0.36	−0.50	−0.01	0.024
ghg + 1.6% clouds (layer 1)	0.98	0.75	0.48	0.51	−0.43	−0.42	−0.55	−0.66	−0.03	0.012
ghg + $2\times\Delta\tau$ (layer 1)	1.38	0.91	0.46	0.62	−0.23	−0.19	−0.24	−0.27	−0.05	0.034
$2\times\Delta\tau$ (layer 7)	0.91	0.44	−0.10	0.51	−0.07	−0.07	−0.02	0.02	−0.04	0.012
ghg + 1.2% clouds + sulfate ($\Delta\tau=0.06$, $\varpi=1.00$)	1.02	0.72	0.41	0.50	−0.37	−0.37	−0.51	−0.75	−0.02	0.013
ghg + R&E sulfate ($\varpi=0.95$) + 1.13% low cloud ($\propto \Delta\tau$)	0.99	0.65	0.62	0.43	−0.30	−0.35	−0.58	−0.86	−0.07	0.025
ghg + R&E sulfate ($\varpi=0.95$) + 1.5%low + 1.5%high clouds	1.03	0.67	0.77	0.40	−0.38	−0.47	−0.81	−1.34	−0.04	0.030

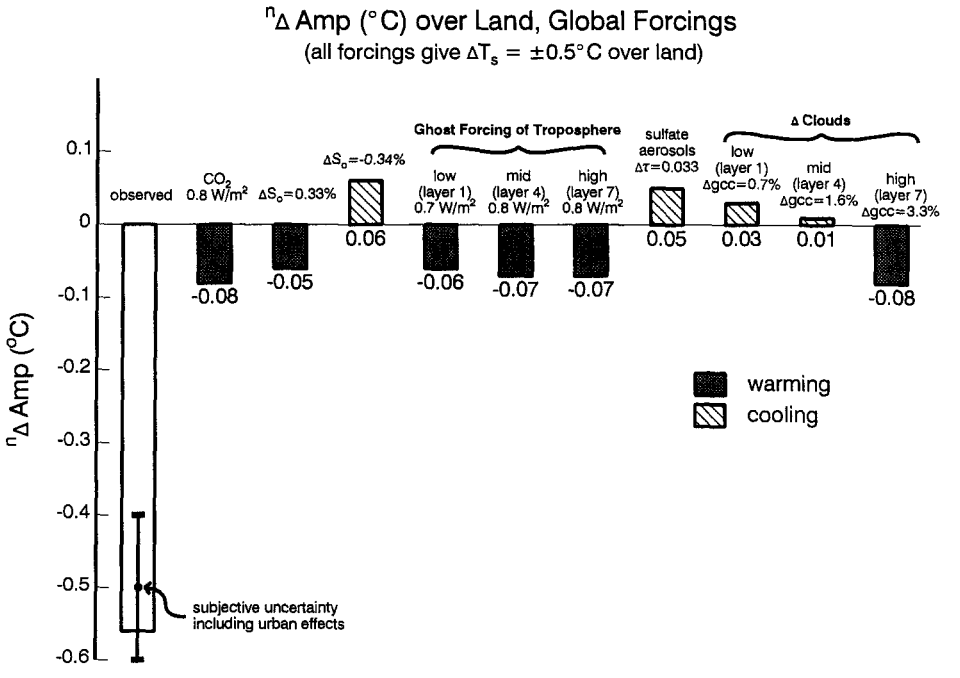

Fig. 14. Equilibrium change of the amplitude of the diurnal cycle of surface air temperature in the Wonderland model for several global climate forcings. Results are scaled to those for a forcing of magnitude required to yield $\Delta T_s = \pm 0.5$°C averaged over land. Clouds are fixed in all of the experiments, but the last three experiments contain specified cloud changes; Δgcc is the cloud cover change in percent of the total area of the Earth.

amplitude of the diurnal cycle of surface air temperature for several global climate forcings. The results in Fig. 14 all refer to the model with fixed clouds. We have normalized the results for each forcing, using Eq. (4), to the response for a temperature change ± 0.5°C averaged over global land.

The "ghost" forcings refer to a heating introduced at arbitrary specified times and places, usually with a global average value of 4 W/m^2. The ghost forcings illustrated in Fig. 14 were introduced in a given atmospheric layer, with the forcing uniform around the globe and constant in time. Layer 1 is the lowest layer of the atmosphere (984–934 mb, on global average), layer 4 is about the middle of the troposphere (720–550 mb) and layer 7 is near the top of the troposphere (255–150 mb).

In tropospheric sulfate aerosol experiments, the aerosols were placed in the lowest three model layers (984–720 mb, on global average; Hansen et al., 1983) with equal optical depths in each layer; because layer thickness increases with height, the aerosols were concentrated toward the ground. Tests with an alternative vertical distribution of aerosols showed no significant change. The aerosol optical depth required to yield an equilibrium global cooling of 0.5°C, about 0.033, can be compared with the optical depth 0.017 estimated by Charlson et al. (1991) as the global mean anthropogenic sulfate amount in 1990. Stratospheric sulfate aerosols yielded the same change of diurnal amplitude, about +0.05°C, as tropospheric aerosols (Table 1).

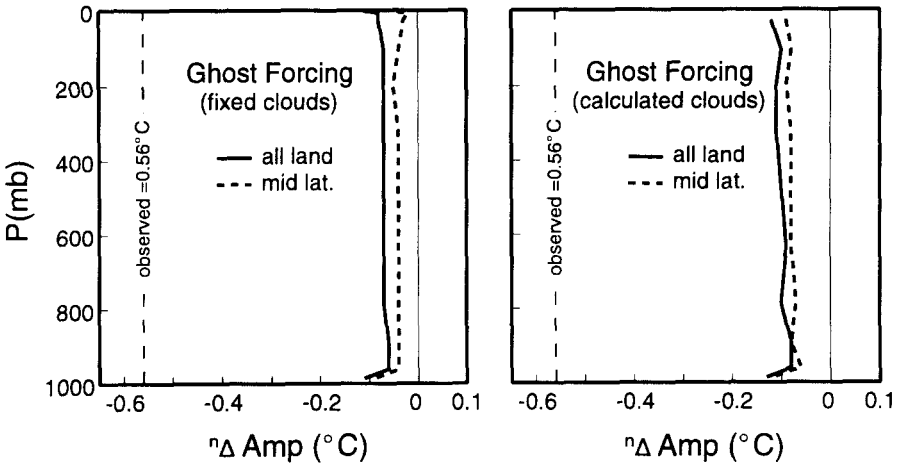

Fig. 15. Change of the amplitude of the diurnal cycle of surface air temperature (normalized to $\Delta T_s = 0.5°C$) in the Wonderland model for a globally uniform "ghost" climate forcing as a function of the pressure level at which the forcing is introduced. Results are shown for both the model with fixed clouds and the model with all feedbacks (water vapor, sea ice and clouds).

The cloud cover changes were made in the regions that were cloud-free in the control run, i.e., in gridboxes without clouds in any layer, thus maximizing the impact of the cloud change. The units for cloud cover (gcc) are the percentage of the total area of the globe, thus, for example, the change of high clouds which yields ΔAmp = −0.08°C reduces the cloud free portion of the model from 45.2% (in the control run) to 41.9%.

The dependence of ΔAmp upon the altitude of the forcing is illustrated in Figs. 15 and 16 for global ghost, ozone and cloud forcings. A 100 year GCM run was made for each forcing inserted individually into each model layer. The ghost forcing was a uniform 4 W/m^2. The ozone forcing was a doubling of ozone in the layer. The cloud forcing was an increase of the clouds in that particular layer such as to reduce the cloud-free fraction of the globe by 5% of the area of the globe. Only two cases yielded $^n\Delta$Amp more than 0.1°C, and both are physically implausible. One case was ozone increase in the lower stratosphere, but the change of $^n\Delta$Amp was only about 0.2°C and the required ozone change (a doubling of the climatological ozone amount in that layer) is unrealistic. The second case was for a cloud increase near the height where albedo cooling and greenhouse warming cancel (between layers 5 and 6, i.e., about 400 mb or 7–8 km), but an implausibly large global cloud cover change would be needed to yield the observed change of diurnal amplitude, as discussed below. Although most of the results we have illustrated are for the model version with fixed clouds, many calculations also were made using the model with calculated clouds, with qualitatively similar results.

The results illustrated in Figs. 12–16 and Table 1 do not reveal any plausible globally uniform climate forcing which can produce a decrease of Amp by 0.5°C while at the same time producing an equilibrium global warming of only 0.5°C. Indeed, with individual globally uniform forcings the discrepancy with observations is about a factor of five.

It is reasonable to ask next whether some combination of these forcings could increase the magnitude of ΔAmp. A promising approach would be to combine a larger amount of

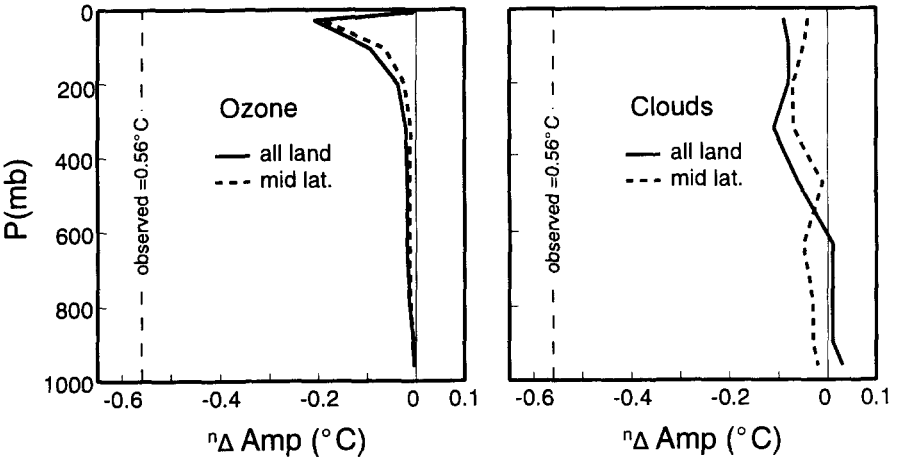

Fig. 16. Change of the amplitude of the diurnal cycle of surface air temperature in the Wonderland model for specified global changes of ozone or cloud cover. The amplitude changes for ozone change refer to a doubling of ozone amount in each layer. Clouds are fixed in all of the model runs, but the experiments on the right include a specified cloud change at a given atmospheric level, scaled to that cloud cover change required to yield a temperature change of ± 0.5°C over land; cloud increase in the lowest 5 layers yields cooling, while cloud increase in layers 6 to 9 causes warming.

greenhouse gases (with a forcing as much as 2 W/m^2 being perhaps conceivable) with an amount of tropospheric aerosols appropriate to limit the global warming to 0.5°C. These changes damp the diurnal cycle by several mechanisms: the aerosols reduce the solar heating, while both the aerosols and the additional greenhouse gases increase the atmospheric infrared opacity, thus reducing nighttime cooling. But quantitative examination reveals that these mechanisms provide little help. The reason is that most of the diurnal damping is due to increasing water vapor, and as long as the global warming is held to 0.5°C the water vapor contribution changes little from one experiment to another. None of the forcings which rely on change of water vapor to decrease Amp yield a change of Amp approaching the observed value, as long as the global temperature increase is only 0.5°C, because the atmospheric temperature exerts such a strong control on the amount of water vapor in the air.

The only apparent mechanism capable of producing such a large change of ΔAmp involves a change of clouds. Indeed, an increase of clouds is often cited as a qualitative explanation for the observed decrease of the diurnal amplitude of surface air temperature. Because of the dominating influence of cloud changes on global average changes of the amplitude of the diurnal cycle, we discuss the impact of cloud changes in some detail.

First consider an increase of low clouds. By itself, an increase of low clouds causes global cooling and increases the amplitude of diurnal surface air temperature variations (Table 1, Figs. 14 and 16). ΔAmp increases because the reduced water vapor more than offsets the fact that added clouds decrease solar heating of the surface and decrease longwave cooling. The only way that a low cloud change can contribute significantly to a reduction of Amp is if the low cloud increase is combined with a larger positive forcing such as increasing greenhouse gases. As an extreme example we first use the 1850–1990 increase of homo-

geneously mixed greenhouse gases (CO_2 285–354 ppm; CH_4 0.80–1.25 ppm; N_2O 285–296 ppb; CFC's as per Hansen et al., 1989), which causes an instantaneous forcing of 2.4 W/m^2, and combine this with an increase of low clouds ($\Delta gcc = 1.2\%$) which reduces the net forcing to 1 W/m^2. The resulting equilibrium normalized change of amplitude averaged over land areas is ${}^n\Delta Amp = -0.15°C$ (Table 1). Thus even with an exaggerated greenhouse forcing [the forcing of these greenhouse gases for the interval 1950–1990 is about 65% of that for the interval 1850–1990 (Hansen et al., 1989)] a global increase of low clouds cannot achieve the observed 0.5°C damping of the diurnal cycle.

Middle level clouds are no more effective at damping the diurnal cycle, if the cloud change is distributed globally. The middle level clouds do not cool the surface as strongly as the low level clouds, and thus it is feasible to add a greater amount of middle level clouds. But the net result of combining middle level clouds with a greenhouse forcing of 2.4 W/m^2 is still only ${}^n\Delta Amp = -0.16°C$ (Table 1).

Next consider an increase of high level clouds, specifically level 7 in the GISS model (255 to 150 mb, about 10 to 14 km), which has cirrus clouds of fixed optical depth 0.33. An increase of such cirrus clouds causes global warming and damps the diurnal cycle. For a global warming of 0.5°C the damping of the diurnal cycle is −0.08°C (Table 1). This is only about the same or slightly greater than the normalized ΔAmp for CO_2 or S_o changes, and far less than observed.

An effective way to achieve a large damping of the diurnal cycle via cloud changes, with a feasible change of net climate forcing, is to combine increases of high clouds and low clouds. An increase of high clouds by $\Delta gcc = 20\%$ (i.e., 20% of the area of the globe) with a low cloud increase of 4% would damp the diurnal amplitude by about 0.5°C. However, this is not a realistic possibility, since a reduction of the cloud free area of the Earth from about 45% to about 20–25% would not have gone unnoticed.

7. More realistic forcings

It is informative to compare the above results, in which none of the known global climate forcings yields a damping of the diurnal cycle approaching the observed changes, to the results of Hansen et al. (1993a), the latter published in Research and Exploration and hereafter referred to as R&E. Although the R&E calculations were carried out with the purpose of determining the expected mean temperature changes for various climate forcings, Hansen et al. (1993a) examined one of the experiments for diurnal cycle changes. With forcings that included greenhouse gases, tropospheric aerosols, and low cloud increases associated with the aerosols, they found that a substantial damping of the diurnal cycle occurred, about −0.25°C averaged over all land and −0.6°C in the region of large aerosol increase (the area labeled "Industrial Region" in Fig. 3).

There are two fundamental differences between the simulations in R&E and those in the earlier sections of this paper. First, the aerosol and cloud forcings in R&E were not globally uniform, but rather were concentrated more heavily over land areas. This difference is the primary factor that increased the damping of the diurnal cycle in the R&E study. Second, the results in R&E were the transient response to a transient forcing, while the above results are the equilibrium response to fixed forcings. This difference has less effect on the mag-

nitude of the diurnal damping, but we show that the mean temperature (ΔT_s) and the diurnal damping (ΔAmp) have different response times, a fact which has important implications.

Forcings over land. Long-lived greenhouse gases, stratospheric aerosols, and solar irradiance changes occur about equally over land and ocean. However, anthropogenic aerosols, and thus also probably anthropogenic cloud changes, are more concentrated over land. Therefore we illustrate first in Fig. 17 and Table 2 the impact of aerosol and cloud changes which are uniform over land and zero over ocean.

A sulfate aerosol optical depth 0.33 over all land yields an equilibrium cooling of -1.5°C over land and damps the diurnal cycle over land by -0.03°C. Normalized to a cooling of -0.5°C over land, requiring an aerosol optical depth 0.11, implies a diurnal amplitude change -0.01°C. Thus this aerosol is able to approximately cancel the increase of the diurnal amplitude which would normally be caused by the water vapor decrease associated with a cooling of 0.5°C. But this aerosol optical depth is much larger than estimates for the real world, and, even if combined with greenhouse warming, aerosols do not yield a damping of the diurnal cycle as great as observed changes.

Cloud changes over land have a large impact on the amplitude of the diurnal cycle over land. For a given change of cloud cover, low clouds cause the greatest decrease of the amplitude of the diurnal cycle (Table 2). However, when normalized to a temperature change over land of 0.5°C (Fig. 17), middle level clouds have a larger impact on the amplitude of the diurnal cycle. High clouds have little direct impact on the diurnal cycle,

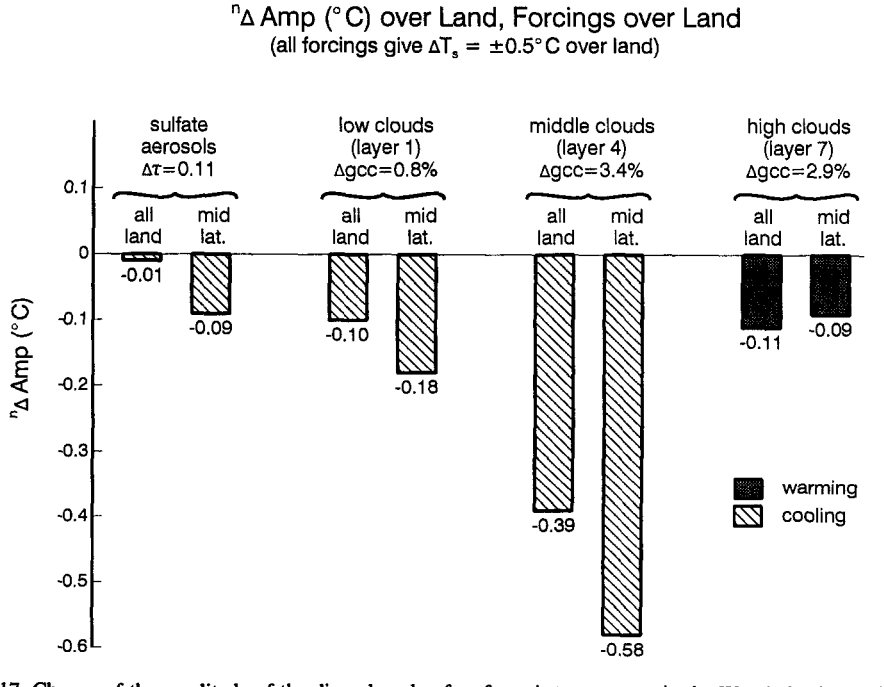

Fig. 17. Change of the amplitude of the diurnal cycle of surface air temperature in the Wonderland model for specified changes of aerosols or clouds over land areas. The model has fixed clouds, except for the specified changes. The results are normalized to a temperature change of ± 0.5°C averaged over land (cf. Eq. 4).

their main influence being through increased water vapor associated with global warming. Although the high clouds in the GISS model have the small optical thickness of mid-latitude cirrus, even if they had the optical depth of low clouds they would be less effective at damping the diurnal cycle because of their low temperature.

Clearly there are different combinations of cloud changes over land which, combined with greenhouse warming, are capable of substantially damping the diurnal cycle. Unfortunately, available cloud observations are not sufficiently accurate to specify actual cloud changes to the required precision. Low clouds are usually assumed to be the most affected by anthropogenic aerosols. But there may also be anthropogenic high cloud changes, for example, as a result of aircraft emissions. Nor can we rule out significant changes of middle level cloud cover, even though such clouds are less abundant than low and high clouds. In the following simulations we consider principally low level cloud changes, because of the considerable evidence about the importance of low level anthropogenic sulfate aerosols and their likely influence on clouds (Charlson et al., 1992).

The combined effects of changes of greenhouse gases, aerosols and clouds are illustrated in Fig. 18 and Table 2. The forcings employed are somewhat larger than expected for the period 1951–1990, in order to provide a good signal-to-noise ratio. The greenhouse gas change, for example, is that estimated for the period 1850–1990 (Hansen et al., 1989), yielding an instantaneous forcing at the tropopause of 2.4 W/m^2 (about 2.1 W/m^2 "adjusted" forcing, if stratospheric temperature is allowed to equilibrate). But the greenhouse forcing for the interval 1951–1990 is almost two-thirds of that for the entire 1850–1990 period, so the forcing is not too inappropriate even for the limited interval of the past four decades. For the sake of obtaining a uniform comparison, we combine the greenhouse gas forcing with the amount of aerosols and/or clouds required to yield a net (instantaneous) forcing of about 1 W/m^2. The use of a net 1 W/m^2 forcing achieves a normalization to a warming close to 0.5°C; simple use of Eqs. (4) and (5) would not be valid for combinations of positive and negative forcings.

The first case in Fig. 18 has global greenhouse gas forcing and tropospheric sulfate aerosols of optical depth 0.25 over land. This combination yields a damping of the diurnal cycle of about 0.3°C over land, but the amount of aerosols is unrealistically large, more than a factor of four larger than the estimate of total present-day anthropogenic sulfate by Charlson et al. (1991); although more recent estimates of anthropogenic aerosol optical depth (Charlson, private commun.) are as much as a factor of two larger than the value of Charlson et al. (1991), a substantial fraction of the anthropogenic component existed already in 1951. The second case, greenhouse gases plus low clouds (Δgcc = 1.6%), yields a damping of about 0.4°C averaged over all land, and 0.55°C at middle latitudes, where most of the observations of diurnal cycle changes are available. The third and fourth cases in Fig. 18 have global greenhouse gases, a realistic aerosol optical depth [0.017 averaged over the globe, the value estimated for anthropogenic sulfates by Charlson et al. (1991), equivalent to about 0.06 over land], and an increase of low level clouds. In the third case the aerosol and cloud changes are distributed uniformly over land, while in the fourth case these changes have a spatial distribution meant to be more characteristic of anthropogenic sulfate (Fig. 10b).

The geographical distributions of the equilibrium ΔT_s and ΔAmp for these same four forcings are shown in Fig. 19. In the three cases which include cloud changes the magnitude

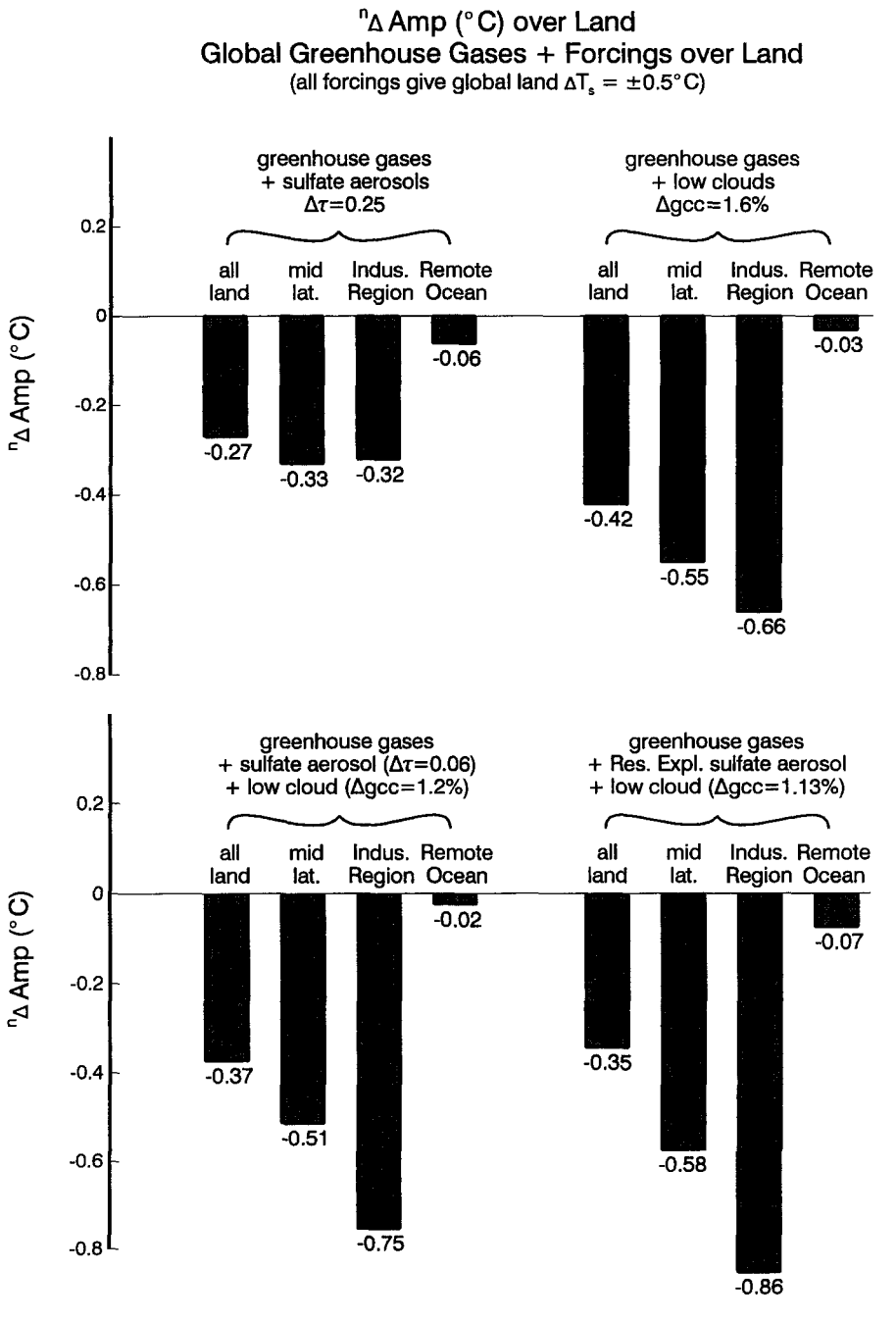

Fig. 18. Change of the amplitude of the diurnal cycle of surface air temperature in the Wonderland model for specified changes of global greenhouse gases plus aerosols and/or clouds over land areas. The net forcing is 1 W/m^2 in all cases. The aerosols and clouds are uniformly distributed over land in the first three cases, and according to the distribution of Fig. 10b in the fourth case.

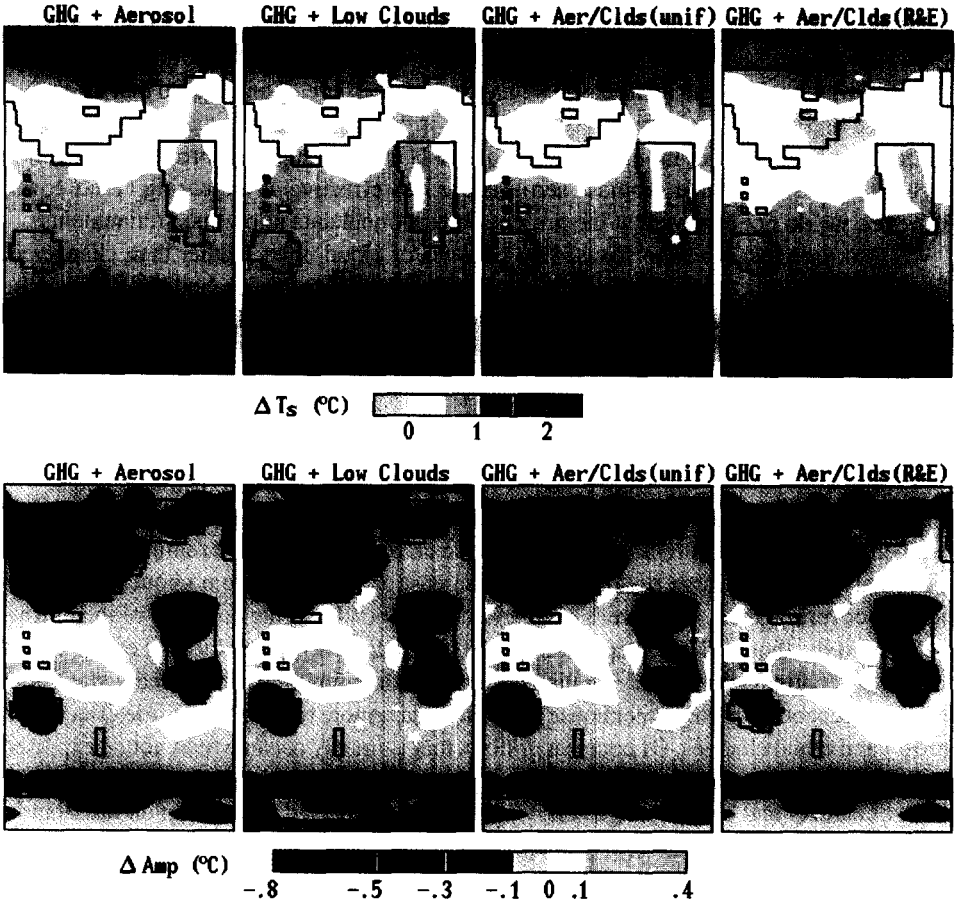

Fig. 19. Equilibrium change of the mean and diurnal amplitude of surface air temperature, ΔT_s and ΔAmp, for the same four climate forcings as in Fig. 18. The net forcing is 1 W/m^2 in all cases. The aerosols and clouds are uniformly distributed over land in the first three cases, and according to the distribution of Fig. 10b in the fourth case.

of the damping of the diurnal cycle is comparable to that observed, of the order of 0.5°C at middle latitudes. ΔAmp is somewhat smaller when averaged over all land (Fig. 18), but given the distribution of observations [figs. 1 and 2 of Karl et al. (1993)], the middle latitude result is perhaps as relevant as the all-land result.

A larger ΔAmp can be obtained by including some middle and high level cloud changes, in addition to the low clouds (Tables 1 and 2). However such refinements are not very meaningful, given the absence of sufficiently precise data on cloud changes. We conclude only that cloud changes over land are capable of damping the diurnal cycle to a degree comparable to observations.

We note that ΔAmp in the last three cases of Fig. 18 is about 0.1°C larger than in the case examined in R&E (Hansen et al., 1993a). The reason is that the case in R&E contained also biomass burning aerosols, with a global mean optical depth equal to that of the sulfate

aerosols; the biomass aerosols were distributed more over the oceans (fig. 16 in R&E), and it was assumed that the biomass aerosols were equally as effective as sulfate at increasing cloud cover. Thus with the constraint of 0.5°C warming over global land, the cloud change over land was smaller than in the cases we have examined here. If one argued that the results in Fig. 18 are closer to observations than those in R&E, it might suggest either that the anthropogenic increase of biomass burning aerosols is less than the anthropogenic increase of sulfate aerosols, or that biomass aerosols are less effective at increasing cloud cover. However, we do not believe that the present observational data allow such refinements.

We also note that we have focused on changes of cloud cover, rather than changes of cloud optical depth. Although it is believed that aerosols influence both of these cloud properties, changes of cloud optical depth have less impact on the diurnal cycle of surface air temperature. This is illustrated by simulations (Table 2) in which we doubled the optical depth of all large scale clouds in layer 1 (''stratus'') and, separately, doubled the optical depth of all large scale clouds in layer 7 (''cirrus''). Increased cloud cover is required to yield the observed magnitude of ΔAmp, but increased cloud optical depth may contribute to the observed damping of Amp, reducing somewhat the needed cloud cover change.

One significant feature in the observed spatial distribution of diurnal cycle changes is the small change observed in remote parts of the ocean. Salinger (1995) examined the change of diurnal cycle for a large region of the ocean east of Australia, from about 10N to 55S latitude, covering about 40 degrees of longitude. He found that the damping of the diurnal cycle was only about 0.1°C, as opposed to the 0.56°C damping found by Karl et al. (1993) for largely continental regions. This is consistent with damping by increased water vapor and homogeneously mixed greenhouse gases at these remote regions, with little effect from aerosol and cloud changes. Of course a gridbox that is mostly ocean would not be expected to show much change in diurnal cycle in any case, averaged over the GCM gridbox, but the effect of aerosol and cloud changes on Amp would be expected to show up on the islands. Thus the small diurnal change observed by Salinger provides a useful confirmation of our interpretation about the continentality of that climate forcing which is principally responsible for large observed diurnal changes.

An anonymous referee requested that we state the aerosol and cloud radiative forcings implied by the observed changes of the diurnal cycle, i.e., the forcings for situations such as those in the lower half of Fig. 18. These cases have an aerosol forcing about $-1/3$ W/m^2 and a cloud forcing about 1 W/m^2. However, this division depends on the assumed aerosol changes; more recent estimates of anthropogenic aerosol amounts imply a larger direct aerosol forcing. Such a change, and transient effects discussed below, reduce the required cloud forcing. Thus we estimate the aerosol forcing as 1/3 to 2/3 W/m^2 (i.e., 0.5 ± 0.17 W/m^2) and the cloud forcing as 0.5–1.0 W/m^2 (i.e., 0.75 ± 0.25 W/m^2). But the cloud forcing would be reduced somewhat if part of the cloud change occurred in the middle or upper troposphere. Accurate determination of the forcings can only be attained with global aerosol and cloud monitoring of high specificity and accuracy, as discussed below.

Transient response. One unrealistic feature of the above simulations is the fact that they each represent the equilibrium response to a fixed forcing, rather than the transient response to transient forcings. The reason for this approach is our desire to isolate the variables for

the sake of analysis, and also to minimize computational requirements. The principal transient effects can be understood in fairly simple ways.

The large thermal inertia of the oceans implies that the response time of the surface air temperature to a given radiative forcing is at least several decades. Thus transient effects are important for surface air temperature, because most of the anthropogenic forcings date from recent decades. Although the response time of the climate system is quite uncertain, because it depends strongly on climate sensitivity, it is estimated that the current (realized) response to anthropogenic greenhouse gases is between about 1/3 and 2/3 of the equilibrium response (Hansen et al., 1985). A useful indication of transient effects on the diurnal cycle can be obtained by examining the intermediate (transient) response in our experiments above with fixed forcings.

Fig. 20 and Table 3 show ΔT_s and ΔAmp at the time the global mean ΔT_s had reached 0.33°C and 0.5°C in several of our simulations with greenhouse gas, sulfate aerosol, and low level cloud changes. The equilibrium ΔT_s in the two cases in Fig. 20 were 0.72°C and 0.65°C. It is apparent that ΔAmp over land areas is nearly independent of time, despite ΔT_s being substantially smaller in the earlier results. The reduction of ΔT_s in the earlier results is more over the oceans than over land, especially in regions of changing sea ice cover.

The time dependences of ΔAmp averaged over all land and ΔT_s averaged over all land and over the globe are shown in Fig. 21. The temperature response over land is substantially delayed by the ocean's thermal inertia, but most of the change of diurnal cycle occurs immediately with the climate forcing, not with the temperature change. The time constant for T_s changes is short, about a decade, in this model which has only a mixed layer ocean. When the deep ocean heat capacity is included the T_s response is further delayed, but most of the Amp change would still occur immediately with the forcing. Only that portion of the Amp change which is due to water vapor change should be delayed and vary with the air temperature over land.

The fact that T_s and Amp have different response times has implications for both our interpretation of past changes of Amp and expectations for future changes. Our analyses based on equilibrium results normalized to a global warming of 0.5°C must be adjusted to account for the likelihood that only about half of the temperature response has been realized for climate forcings added during this century; of course the R&E analyses, with transient forcings and transient simulations, do not require such adjustment. The quantitative conclusion is that increasing greenhouse gases and tropospheric aerosols can account for as much as one third to one half of the observed damping of the diurnal cycle. The increased cloud cover required to account for the remaining observed change of Amp is Δgcc $= 1 \pm 0.5\%$ if the changes are principally low clouds, corresponding to an increased sky cover by clouds of 2–5% over affected land regions.

The transient results of Table 3 also allow us to compare the relative warmings in the two hemispheres with observations. The observations (e.g., fig. 8 of Balling, 1993) show that the Southern Hemisphere warmed about 0.2°C more than the Northern Hemisphere during the past four decades. With the aerosol and cloud forcings in our simulations, which are either proportional to land area or even more heavily weighted toward the Northern Hemisphere (with the R&E sulfate distribution), the relative hemispheric temperature change by the time the global warming reaches 0.33°C (approximately the global warming in the period 1951–1990) is of the observed sign and of a magnitude comparable to that

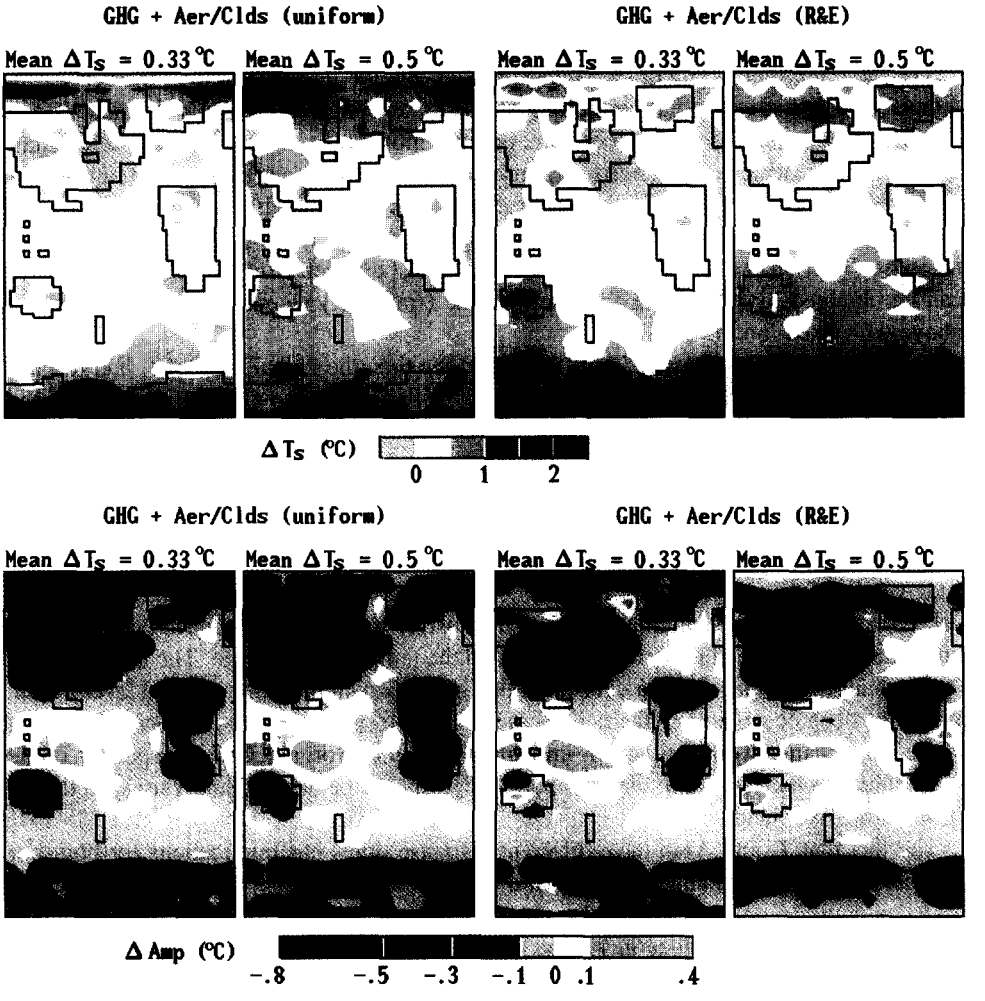

Fig. 20. Non-equilibrium change of the mean and diurnal amplitude of surface air temperature, ΔT_s and ΔAmp, for two of the climate forcings of Fig. 18. The results are averages over several years at the times when the global warming had reached 0.33°C and 0.5°C. The aerosols and clouds are uniformly distributed over land in the case shown on the left and according to the distribution of Fig. 10b in the case on the right.

observed. We certainly do not take this as a confirmation of the forcings, because the uncertain factors are too great (e.g., the model results depend on the accuracy of the sea ice feedback, and also unrepresented feedbacks in the ocean dynamics could alter the results), but rather as an indication that there is no great inconsistency with observations of the hemispheric responses.

Finally, we note that recent observations of differences in the trends of Amp at midland and Alpine locations (Weber et al., 1994) are consistent with the conclusion that anthropogenic aerosols and low cloud changes are mainly responsible for the damping of Amp. Of course it is inappropriate to infer too much from observations in a single region. Confident

Table 3
Transient changes of surface air temperature and diurnal cycle parameters in GCM experiments with a variety of inhomogeneously distributed radiative forcings. The "land" results are the mean for all land in Wonderland excluding the ice-covered continents Whiteland and Friesland. Values are shown for transient periods, averaged over several years, by which time global mean warming reached either 0.33°C or 0.5°C

	ΔT_s			ΔAmp				ΔAsym
Experiment	Global	SH-NH	All land	All land	Mid lat.	Indus. region	Remote ocean	All land
ghg + sulfate	0.33	0.16	0.25	−0.26	−0.23	−0.18	−0.02	0.019
($\Delta\tau$=0.25)	0.50	0.30	0.30	−0.29	−0.29	−0.29	−0.02	0.025
ghg + low clouds	0.33	0.22	0.19	−0.42	−0.53	−0.64	—	0.029
(Δgcc = 1.6%)	0.50	0.19	0.39	−0.46	−0.58	−0.78	—	0.031
ghg + sulfate	0.33	0.12	0.24	−0.38	−0.55	−0.77	−0.04	0.008
($\Delta\tau$=0.06)	0.50	0.16	0.39	−0.39	−0.54	−0.71	−0.03	0.010
+ low clouds								
(Δgcc = 1.2%)								
ghg + R&E sulfate	0.33	0.39	0.24	−0.24	−0.46	−0.78	−0.06	0.012
aerosols	0.50	0.49	0.32	−0.30	−0.53	−0.90	−0.05	0.020
+ low clouds								
(Δgcc = 1.13%)								

interpretation will only be possible if the aerosol and cloud changes themselves are measured, with the necessary precision, as discussed below.

8. Discussion

Principal conclusions. The large observed damping of the diurnal cycle of surface air temperature implies the existence of a substantial climate forcing located in continental regions. Anthropogenic aerosols can account for only part of this forcing; the remainder can only be provided by increased cloud cover. The magnitude of the required cloud increase, Δgcc ∽ 1% for low clouds, corresponds to an increase of sky coverage of 2 ~ 5% over land (i.e., from, say, 55% to 57–60%). Ground-based observations of cloud cover are not inconsistent with such a cloud change (Henderson-Sellers, 1989; McGuffie and Henderson-Sellers, 1993), but the spatial coverage and long-term precision of the data are inadequate for quantitative studies.

Needed observations. The climatic implications of such cloud and aerosol changes can be discerned only if the changes are known globally on decadal time scales. The required long-term precision of measurement required to interpret decadal climate change are a cloud cover change Δgcc = 0.4% as a function of cloud height (Δp = 5 mb) and a tropospheric aerosol optical depth change $\Delta\tau$ = 0.01 (chapter 7, table 7.4, Hansen et al., 1993b); not coincidentally, these same precisions are required for understanding of the diurnal cycle changes. Although such precisions are not attained by existing or flight-scheduled satellite instruments, the capabilities have been demonstrated with relatively inexpensive long-lived planetary instruments. Specifically, a Michelson interferometer (Hanel et al., 1980) has

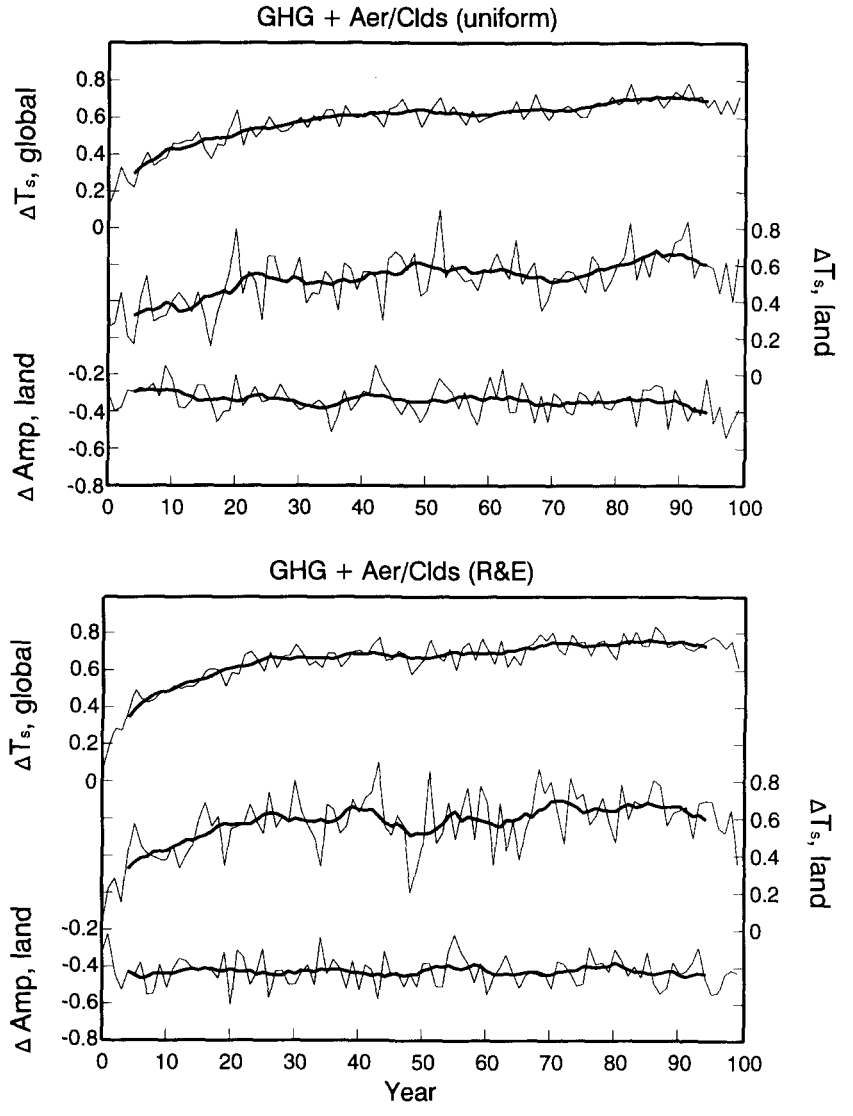

Fig. 21. Time dependence of ΔAmp averaged over all land and ΔT_s averaged over all land and averaged over the globe. The aerosols and clouds are uniformly distributed over land in the top case and according to the distribution of Fig. 10b in the bottom case.

been shown to be capable of the cloud measurements in a multilayered atmosphere (Carlson et al., 1993). Similarly, a photopolarimeter has been demonstrated to be capable of such precise aerosol measurements (Travis, 1992), including accurate determination of aerosol and cloud microphysical properties. Without such data, long-term global climate forcings will remain unknown and interpretation and projection of any observed global climate change will be impossible.

Implications. Our analysis of the observed change of the amplitude of the diurnal temperature cycle leads to the conclusion that there has been a substantial negative climate forcing over the past four decades, including an increase of cloud cover. Although the data do not allow the forcing to be pinpointed, the simplest interpretation is that low clouds have increased in association with increasing anthropogenic sulfate aerosols. In that case, the net forcing by aerosol and cloud changes required to yield the observed damping of the diurnal cycle is about half as large as the anthropogenic greenhouse gas climate forcing, and of the opposite sign. Perhaps not coincidentally, reduction of greenhouse gas forcing by about one half is required for climate models to yield best agreement with observed warming of the past century, if climate is as sensitive as indicated by paleoclimate data (Wigley, 1991; Schlesinger et al., 1992; Hansen et al., 1993a).

The existence of this negative climate forcing represents a problem for policy makers, in the absence of more precise identification and measurement of the forcing. Aerosols and aerosol-induced cloud changes may arise chiefly from fossil fuel burning, the activity which is also mainly responsible for increase of atmospheric carbon dioxide. Thus the impact of policies related to fossil fuel use on the net climate forcing can be assessed reliably only with quantitative understanding of the aerosol and cloud forcings, as well as the greenhouse gas forcing. Comparison of the greenhouse gas and aerosol/cloud forcings is further complicated by the very different spatial distributions of these forcings, which implies that they can not cause a simple cancellation.

Finally, we note that the claim made by "greenhouse critics" in the popular press, that global warming is a "benign" nighttime phenomenon, is incorrect. The temperature changes, as we have shown, represent the combination of an overall warming and a damping of the diurnal cycle. We can safely predict that on the long run the effect of the diurnal damping on maximum temperatures will be small, for the following three reasons. First, even during the past four decades the 0.56°C damping of the diurnal cycle did not eliminate daytime warming, but rather reduced it from 0.56°C to 0.28°C. Second, as illustrated by Fig. 21, almost all of the damping caused by a climate forcing occurs immediately with the introduction of the forcing, while the mean temperature rise is delayed by the thermal inertia of the climate system. Thus the unrealized warming for greenhouse gases already in the atmosphere will appear almost equally in daily maximum and daily minimum temperatures. Third, as anthropogenic emissions level off the forcings which principally damp the diurnal cycle, aerosol and cloud changes, will level off, but the long-lived greenhouse gases will continue to accumulate. Thus, except for the small damping due to increased water vapor, the maximum temperature should increase as fast as the minimum temperature. Empirical evidence for our conclusion about maximum temperature could be provided by the occurrence of daily maximum temperature records at a frequency exceeding statistical expectations.

Acknowledgements

Peter Stone, David Parker, Shaw Liu and two anonymous referees provided useful suggestions on the first draft of the manuscript. We thank Jeffrey Jonas and Christina Koizumi for technical support with the graphics and desktop typesetting. Gary Russell

provided the data for Fig. 2, comparing the observed and modeled diurnal cycle. This work was supported by the NASA Climate, Earth Observing System and Tropospheric Aerosol Research programs.

References

Angell, J.K., 1986. Annual and seasonal global temperature changes in the troposphere and low stratosphere, 1960–1985. Mon. Weather Rev., 114: 1922–1930.

Angell, J.K., 1991. Changes in tropospheric and stratospheric global temperatures, 1958–1988. In: M.E. Schlesinger (Editor), Greenhouse-Gas-Induced Climatic Change. Elsevier, Amsterdam, pp. 231–247.

Balling, R.C., 1993. The global temperature data. Nat. Geogr. Res. Explor., 9: 201–207.

Cao, H.X., Mitchell, J.F.B. and Lavery, J.R., 1992. Simulated diurnal range and variability of surface temperature in a global climate model for present and doubled CO_2 climates. J. Clim., 5: 920–943.

Carlson, B.E., Lacis, A.A. and Rossow, W.B., 1993. Tropospheric gas composition and cloud structure of the Jovian North Equatorial Belt. J. Geophys. Res., 98: 5251–5290.

Charlson, R.J., Langner, J., Rodhe, H., Leovy, C.B. and Warren, S.G., 1991. Perturbation of the Northern Hemisphere radiative balance by back-scattering from anthropogenic sulfate aerosols. Tellus, 43AB: 152–163.

Charlson, R.J., Schwartz, S.E., Hales, J.M., Cess, R.D., Coakley, J.A., Hansen, J.E. and Hofmann, D.J., 1992. Climate forcing by anthropogenic aerosols. Science, 255: 423–430.

Hanel, R., Crosby, D., Herath, L., Vanous, D., Collins, D., Creswick, H., Harris, C. and Rhodes, M., 1980. Infrared spectrometer for Voyager. Appl. Opt., 19: 1391–1400.

Hansen, J. and Lebedeff, S., 1987. Global trends of measured surface air temperature. J. Geophys. Res., 92: 13,345–13,372.

Hansen, J., Russell, G., Rind, D., Stone, P., Lacis, A., Lebedeff, S., Ruedy, R. and Travis, L., 1983. Efficient three-dimensional models for climate studies: models I and II. Mon. Weather Rev., 111: 609–662.

Hansen, J., Lacis, A., Rind, D., Russell, G., Stone, P., Fung, I., Ruedy, R. and Lerner, J., 1984. Climate sensitivity: analysis of feedback mechanisms. In: J.E. Hansen and T. Takahashi (Editors), Climate Processes and Climate Sensitivity. Geophys. Monogr. Ser., 29. AGU. Washington, D.C., pp. 130–163.

Hansen, J., Russell, G., Lacis, A., Fung, I., Rind, D. and Stone, P., 1985. Climate response times: dependence on climate sensitivity and ocean mixing. Science, 229: 857–859.

Hansen, J., Lacis, A. and Prather, M., 1989. Greenhouse effect of chlorofluorocarbons and other trace gases. J. Geophys. Res., 94: 16,417–16,421.

Hansen, J., Lacis, A., Ruedy, R., Sato, M. and Wilson, H., 1993a. How sensitive is the world's climate? Nat. Geogr. Res. Explor., 9: 142–158.

Hansen, J., Rossow, W. and Fung, I., 1993b. Long-Term Monitoring of Global Climate Forcings and Feedbacks. NASA CP 3234, Proc. workshop held at Goddard Institute for Space Studies, New York, February 3–4, 1992, 91 pp.

Hansen, J., Ruedy, R., Russell, G., Lerner, J., Sato, M., Lacis, A., Rind, D. and Stone, P., 1995a. Wonderland climate model. J. Geophys. Res. (to be submitted).

Hansen, J., Sato, M. and Ruedy, R., 1995b. Radiative forcings and climate response. J. Geophys. Res. (to be submitted).

Henderson-Sellers, A., 1989. North American total cloud amount variations in this century. Global Planet. Change, 1: 175–194.

IPCC (Intergovernmental Panel on Climate Change), 1990. Climate Change. In: J.T. Houghton, G.J. Jenkins and J.J. Ephraums (Editors), The IPCC Scientific Assessment. Cambridge University Press, 365 pp.

IPCC (Intergovernmental Panel on Climate Change), 1992. Climate Change 1992. In: J.T. Houghton, B.A. Callander and S.K. Varney (Editors), The Supplementary Report to the IPCC Scientific Assessment. Cambridge University Press, 200 pp.

Jones, P.D., Wigley, T.M.L., and Farmer, G., 1991. Marine and land temperature data sets: a comparison and a look at recent trends. In: M.E. Schlesinger (Editor), Greenhouse-Gas-Induced Climatic Change. Elsevier, Amsterdam, pp. 153–172.

Karl, T.R., Jones, P.D., Knight, R.W., Kukla, G., Plummer, N., Razuvayev, V., Gallo, K.P., Lindseay, J., Charlson, R.J. and Peterson, T.C., 1993. A new perspective on recent global warming. Bull. Am. Meteorol. Soc., 74: 1007–1023.

Kukla, G. and Karl, T.R., 1993. Nighttime warming and the greenhouse effect. Environ. Sci. Tech., 27: 1468–1474.

Kumar, K.R., Kumar, K.K. and Pant, G.B., 1994. Diurnal asymmetry of surface temperature trends over India. Geophys. Res. Lett., 21: 677–680.

Lacis, A.A., Wuebbles, D.J. and Logan, J.A., 1990. Radiative forcing of climate by changes of the vertical distribution of ozone. J. Geophys. Res., 95: 9971–9981.

Manabe, S., 1969. Climate and ocean circulation: I. The atmospheric circulation and the hydrology of the Earth's surface. Mon. Weather Rev., 97: 739–774.

Manabe, S. and Wetherald, R.T., 1975. The effects of doubling the CO_2 concentration on the climate of a general circulation model. J. Atmos. Sci., 32: 3–15.

May, W., Shea, D. and Madden, R.A., 1992. The Annual Variation of Surface Temperatures over the World. NCAR Tech. Note, NCAR/TN-372 + STR, Boulder.

McGuffie, K. and Henderson-Sellers, A., 1993. Cloudiness trends this century from surface observations. Minimax Workshop Extended Abstracts, College Park, Maryland, September 27–30, pp.

Miller, R.L. and DelGenio, A.D., 1994. Tropical cloud feedbacks and natural variability of climate. J. Clim., 7: 1383–1402.

Oort, A.H., 1993. Observed humidity trends in the atmosphere. NOAA, Proc. 17th Annu. Climate Diagnostics Workshop, held at Norman, Oklahoma, October 19–23, 1992, pp. 24–30.

Oort, A.H. and Liu, H., 1993. Upper-air temperature trends over the globe, 1958–1989. J. Clim., 6: 292–307.

Salinger, M.J., 1995. Southwest Pacific temperatures: trends in maximum and minimum temperatures. Atmos. Res. (this issue).

Schlesinger, M.E., Jiang, X. and Charlson, R.J., 1992. Implication of anthropogenic atmospheric sulfate for the sensitivity of the climate system. In: L. Rosen and R. Glasser (Editors), Climate Change and Energy Policy. Am. Inst. Phys., New York, pp. 75–108.

Travis, L.D., 1992. Remote sensing of aerosols with the Earth Observing Scanning Polarimeter. Proc. Polarization and Remote Sensing, Vol. 1747, SPIE, San Diego, pp. 154–164.

Weber, R.O., Talkner, P. and Stefanicki, G., 1994. Asymmetric diurnal temperature change in the Alpine region. Geophys. Res. Lett., 21: 673–676.

Wetherald, R.T. and Manabe, S., 1975. The effects of changing the solar constant on the climate of a general circulation model. J. Atmos. Sci., 32: 2044–2059.

Wigley, T.M.L., 1991. Could reducing fossil-fuel emissions cause global warming? Nature, 349: 503–506.